The Effects and Mechanisms of Action of TC-G 1008, GPR39 Agonist, in Animal Models of Seizures and Epilepsy

Urszula Doboszewska (urszula.doboszewska@umcs.lublin.pl)
Maria Curie-Sklodowska University: Uniwersytet Marii Curie-Sklodowskiej https://orcid.org/0000-0002-2700-8155

Katarzyna Socala
Maria Curie-Sklodowska University: Uniwersytet Marii Curie-Sklodowskiej

Mateusz Pieróg
Maria Curie-Sklodowska University: Uniwersytet Marii Curie-Sklodowskiej

Dorota Nieoczym
Maria Curie-Sklodowska University: Uniwersytet Marii Curie-Sklodowskiej

Jan Sawicki
Medical University of Lublin: Uniwersytet Medyczny w Lublinie

Małgorzata Szafarz
Jagiellonian University: Uniwersytet Jagiellonski w Krakowie

Kinga Gaweł
Medical University of Lublin: Uniwersytet Medyczny w Lublinie

Anna Rafalo-Ulińska
Institute of Pharmacology of the Polish Academy of Sciences: Instytut Farmakologii im Jerzego Maja Polskiej Akademii Nauk

Elżbieta Wyska
Jagiellonian University: Uniwersytet Jagiellonski w Krakowie

Camila V. Esguerra
University of Oslo: Universitetet i Oslo

Bernadeta Szewczyk
Institute of Pharmacology of the Polish Academy of Sciences: Instytut Farmakologii im Jerzego Maja Polskiej Akademii Nauk

Marzena Maćkowiak
Institute of Pharmacology of the Polish Academy of Sciences: Instytut Farmakologii im Jerzego Maja Polskiej Akademii Nauk

Katarzyna Młyniec
Jagiellonian University: Uniwersytet Jagiellonski w Krakowie

Gabriel Nowak

Institute of Pharmacology of the Polish Academy of Sciences: Instytut Farmakologii im Jerzego Maja Polskiej Akademii Nauk

Ireneusz Sowa

Medical University of Lublin: Uniwersytet Medyczny w Lublinie

Piotr Wlaź

Maria Curie-Sklodowska University: Uniwersytet Marii Curie-Sklodowskiej

---

Research Article

Keywords: GPR39, TC-G 1008, seizure, epilepsy, intracellular zinc

Posted Date: January 7th, 2022

DOI: https://doi.org/10.21203/rs.3.rs-1182423/v1

The effects and mechanisms of action of TC-G 1008, GPR39 agonist, in animal models of seizures and epilepsy

Urszula Doboszewska[1*], Katarzyna Socała[1], Mateusz Pieróg[1], Dorota Nieoczym[1], Jan Sawicki[2], Małgorzata Szafarz[3], Kinga Gaweł[4], Anna Rafało-Ulińska[5], Elżbieta Wyska[3], Camila V. Esguerra[6], Bernadeta Szewczyk[5], Marzena Maćkowiak[7], Katarzyna Młyniec[8], Gabriel Nowak[5,8], Ireneusz Sowa[2], Piotr Wlaź[1]

[1]Department of Animal Physiology and Pharmacology, Institute of Biological Sciences, Maria Curie-Skłodowska University, Akademicka 19, PL 20-033 Lublin, Poland

[2]Department of Analytical Chemistry, Medical University of Lublin, Chodzki 4A, PL 20-093 Lublin, Poland

[3]Department of Pharmacokinetics and Physical Pharmacy, Jagiellonian University Medical College, Medyczna 9, PL 30-688 Kraków, Poland

[4]Department of Experimental and Clinical Pharmacology, Medical University of Lublin, Jaczewskiego 8b, 20-090 Lublin, Poland

[5]Department of Neurobiology, Maj Institute of Pharmacology, Polish Academy of Sciences, Smetna 12, PL 31-343 Krakow, Poland

[6]Chemical Neuroscience Group, Centre for Molecular Medicine Norway, University of Oslo, Gaustadalléen 21, Forskningsparken, 0349 Oslo, Norway

[7]Laboratory of Pharmacology and Brain Biostructure, Department of Pharmacology, Maj Institute of Pharmacology, Polish Academy of Sciences, Smetna 12, PL 31-343 Krakow, Poland

[8]Department of Pharmacobiology, Jagiellonian University Medical College, Medyczna 9, PL 30-688 Kraków, Poland

*Corresponding author: Department of Animal Physiology and Pharmacology, Institute of Biological Sciences, Faculty of Biology and Biotechnology, Maria Curie-Sklodowska University, Akademicka 19, PL 20-033 Lublin, Poland. Phone: +48 81 537-50-10, Fax: +48 81 537-59-01; E-mail address: urszula.doboszewska@umcs.lublin.pl (U. Doboszewska); Present address: Department of Pharmacobiology, Jagiellonian University Medical College, Kraków, Poland, e-mail address: urszula.doboszewska@uj.edu.pl

ORCID identifiers:

Urszula Doboszewska: 0000-0002-2700-8155

Katarzyna Socała: 0000-0001-7706-2080

Mateusz Pieróg: 0000-0001-8772-3225

Dorota Nieoczym: 0000-0002-9446-7343

Jan Sawicki: 0000-0002-5945-1047

Małgorzata Szafarz: 0000-0002-8619-5659

Kinga Gawel: 0000-0001-8857-847X

Anna Rafalo-Ulińska: 0000-0001-7576-8039

Elżbieta Wyska: 0000-0002-4798-0574

Camila V. Esguerra: 0000-0002-2271-8094

Bernadeta Szewczyk: 0000-0002-6863-7951

Marzena Maćkowiak: 0000-0002-6056-9595

Katarzyna Mlyniec: 0000-0002-9257-8154

Gabriel Nowak: 0000-0002-3000-7938

Ireneusz Sowa: 0000-0001-9346-6325

Piotr Wlaź: 0000-0002-5389-0241

Abstract

Background and purpose: The G-protein coupled receptor 39 (GPR39) may be activated by zinc ions. Activation of GPR39 was suggested as a novel pharmacological strategy for treating seizures. Experimental approach: We utilized a specific agonist of GPR39, TC-G 1008, and the nonspecific agonist, zinc chloride and a variety of models of acute seizures or a chronic model of epilepsy which were induced in non-genetically modified mice, GPR39 knockout mice or in zebrafish larvae. We examined total serum zinc (by Inductively Coupled Plasma Optical Emission Spectrometry) as well as intracellular zinc ($[Zn^{2+}]_I$) (by Zinpyr-1 staining) concentrations and the expression of selected proteins (by Western blot) which are associated with GPR39 signaling in the hippocampus. Key results: Liquid chromatography tandem mass spectrometry analysis showed that TC-G 1008 is brain penetrant. TC-G 1008 decreased the seizure threshold in the maximal electroshock seizure (MES) threshold test, but it increased the seizure threshold in the 6-Hz induced seizure threshold test. The behavioral effects of TC-G 1008 and MES or 6-Hz seizure were accompanied by alterations in hippocampal $[Zn^{2+}]_I$. TC-G 1008 increased the mean duration of EEG discharges in response to pentylenetetrazole (PTZ) in zebrafish larvae and facilitated the development of PTZ kindling in mice. Using GPR39 knockout mouse line, generated by the CRISPR-Cas-9 method, we showed that GPR39 is a target for TC-G 1008 regarding PTZ-induced epileptogenesis. Conclusion and implications: Our in vivo data obtained using TC-G 1008 generally argue against GPR39 activation as a therapeutic strategy for alleviating seizures/epilepsy.

Keywords: GPR39, TC-G 1008, seizure, epilepsy, intracellular zinc

Introduction

Epilepsy is one of the most prevalent neurological diseases, affecting more than 65 million people worldwide [1]. The disease can be controlled pharmacologically, but more than one third of patients remain treatment-resistant [2]. The available drugs suppress only symptoms of epilepsy, *i.e.*, either stop or reduce the frequency or severity of seizures, but they do not interfere with the process of epilepsy development, *i.e.*, epileptogenesis [3]. It is therefore crucial to find novel drug targets and develop new compounds that will not only inhibit seizures but also possess antiepileptogenic properties [4].

Most of zinc ions are bound to proteins but the small pool of "free" or "labile" zinc is available for signaling, which occurs both intracellularly and extracellularly [5]. Although studies did not provide direct intracellular/extracellular concentrations of zinc ions associated with seizures, a link between increased intracellular "free" zinc concentration ($[Zn^{2+}]_I$) and status epilepticus (SE), which is a risk factor for epilepsy [6], was demonstrated [7]. The neuromodulatory function of extracellular zinc on numerous targets that mediate neuronal excitation or inhibition was shown to be of importance in terms of seizures/epilepsy [8]. In addition, extracellular zinc was suggested to activate a G-protein-coupled receptor (GPCR), namely GPR39 [9, 10]. The existence of a GPCR activated by zinc ions was postulated before [11] although there is still debate whether the physiological/ pathophysiological concentrations of zinc are sufficient to activate the receptor [12] and whether zinc is the only one agonist [13].

GPR39 is increasingly gaining attention as a target for future drugs in several therapeutic areas, including the central nervous system [14-16]. GPR39 knockout (KO) mice displayed enhanced susceptibility to seizures triggered by a single intraperitoneal (*i.p.*) injection of kainic acid (KA), compared with wild-type (WT) littermates [17, 18]. Lithium chloride-pilocarpine-induced-SE decreased the expression of GPR39 at the protein level in the

hippocampus [19]. RNA sequencing revealed up-regulation of the *gpr39* gene in *stim2b* knockout zebrafish, which is hyperactive and more sensitive to treatment with pentylenetetrazole (PTZ) [20]. These data suggested the association between GPR39 and seizures. The involvement of GPR39 in epileptogenesis has not been examined.

We hypothesized that the activation of GPR39 may reduce seizures and/or produce an antiepileptogenic effect. To test this hypothesis *in vivo*, we administered GPR39 agonist, TC-G 1008 (compound 3 [21], GPR39-C3 [22]) and the nonspecific agonist, zinc chloride ($ZnCl_2$) in mice and zebrafish larvae. We compared their effects to that of a standard antiseizure drug, valproic acid (VPA). Our first aim was to assess the behavioral or electroencephalographic (EEG) effects in acute seizure tests or a chronic model reflecting epileptogenesis. Our second aim was to assess the response of GPR39 KO mice to seizure-inducing/ epileptogenic agents and treatment with TC-G 1008, thus gaining more insights into the phenotype of GPR39 KO mice and the physiological role of GPR39. We also examined whether the effects of TC-G 1008 or GPR39 KO are accompanied by alterations in $[Zn^{2+}]_I$ or expression of proteins of the GPR39 signaling pathway.

Methods

Materials

TC-G 1008 was purchased from Adooq Bioscience LLC (Irvine, CA, USA). VPA (sodium salt), $ZnCl_2$, PTZ and KA were obtained from Sigma-Aldrich. For experiments in mice, $ZnCl_2$, VPA, PTZ and KA were dissolved in physiological saline (0.9% sodium chloride (NaCl) solution). TC-G 1008 was suspended in 1% Tween 80 solution in physiological saline. For experiments in zebrafish, $ZnCl_2$ and TC-G 1008 were dissolved in embryo medium. PTZ was dissolved to 60 mM (3x stock) in embryo medium. The materials used for biochemical analyses are listed in the sections on Liquid Chromatography Tandem Mass Spectrometry (LC-MS/MS), Western blot, Inductively Coupled Plasma Optical Emission Spectrometry (ICP-OES) or Zinpyr-1 (ZP-1) staining.

Animals

The experiments were performed in non-genetically modified mice, GPR39 KO mice and in zebrafish (*Danio rerio*) larvae. Housing and experimental procedures were conducted in accordance with the European Union Directive of 22 September 2010 (2010/63/EU), and Polish and Norwegian legislation acts concerning animal experimentation. The experiments in mice were approved by the Local Ethical Committee in Lublin (experiments in non-genetically modified mice: approval numbers 38/2017, 48/2018, 110/2018, 36/2019; experiments in GPR39 KO mice: approval numbers 72/2019, 16/2020), and the I Local Ethical Committee in Warsaw (approval number 811/2019 regarding generation of the GPR39 KO mouse line). The experiments in zebrafish were approved by the Norwegian Food Safety Authority experimental animal administration's supervisory and application system (“Forsøksdyrforvatningen tilsyns- og søknadssystem”; FOTS ID 15469 and 23935). All efforts were made to minimize animal suffering as well as the number of animals used in the

study. During the experiments, the animals were closely followed-up by the animal caretakers and researchers, with regular inspection by a veterinarian, according to the standard health and animal welfare procedures of the local animal facility.

Experimentally naïve male Swiss Albino mice (n=966) with a body weight range of 17–31 g, were purchased from a licensed breeder (Laboratory Animals Breeding, Ilkowice, Poland) and were housed in an animal house at the Faculty of Biology and Biotechnology of Maria Curie Sklodowska University in Lublin, in groups of 7-8 in open Makrolon cages (37 cm × 21 cm × 14 cm) under strictly controlled laboratory conditions (temperature maintained at 21–24 °C, relative humidity at 45–65%) with an artificial 12/12 h light/dark regime (light on at 6:00 a.m.). A rodent chow diet (Murigran, Agropol S.J., Motycz, Poland) and tap water were provided *ad libitium*. The environment was enriched with nest material and paper tubes.

GRP39 KO mouse model was generated by the Mouse Genome Engineering Facility (crisprmice.eu). A CRISPR/Cas 9 method was used to establish the model in mixed genetic background (C57BL/6/Tar x CBA/Tar). A deletion of 44 bp causing p.Lys38fs*57X frameshift mutation was introduced. WT and KO mice were housed in an animal house at the Experimental Medicine Center of the Medical University in Lublin. Male WT mice (n=35) and male KO mice (n=35) with a body weight range of 16-29 g were used for experiments. The mice were housed in groups of 7-8 in open Makrolon cages (37 cm × 21 cm × 14 cm) under strictly controlled laboratory conditions (temperature maintained at 21–24 °C, relative humidity at 45–65%) with an artificial 12/12 h light/dark regime (light on at 6:00 a.m.). The diet (Altromin standard diet, Altromin, Lage, Germany) and tap water were provided *ad libitium*. The environment was enriched with nest material and paper tubes. Only male Swiss Albino or C57BL/6/Tar x CBA/Tar mice were used to exclude the possible impact of the estrous cycle on seizure susceptibility [23].

The following procedures were performed in Swiss Albino mice: determination of TC-G 1008 concentration in serum and brain, maximal electroshock seizure (MES) threshold test (MEST), MES generated by supramaximal stimulus of 50 mA, 6-Hz-induced seizure threshold test, 6-Hz seizure generated by supramaximal current intensity of 32 mA, intravenous (*i.v.*) PTZ seizure threshold test, acute KA-induced seizure, PTZ kindling and biochemical analyses. The following procedures were performed in C57BL/6/Tar x CBA/Tar GPR39 KO and WT mice: the MEST test, PTZ kindling and biochemical analyses. Animals were randomly assigned to the experimental groups. Blinding was not feasible during behavioral experiments due to the rotations of experimenters who either administered compounds or observed their behavioral effects. Blinding was applied during biochemical analyses.

All procedures in mice begun after at least one week of acclimatization and were performed between 8:00 a.m. to 3:00 p.m., after a minimum 30-min adaptation period to the conditions in the experimental room. Drug solutions/suspensions were prepared freshly and administered i.p. at a volume of 0.1 ml per 10 g of body weight. Control groups received vehicles (VEH) used for the preparation of drug solutions/suspensions. The drugs were administered 30 min before acute seizure tests or acute seizure models or before PTZ/KA injections. This pretreatment time was chosen after determination of TC-G 1008 concentrations in serum and brain (Fig 1). With the exception of 1% ophtalmic solution of tetracaine, which was used for a short-term topical ophthalmic anesthesia before determining the seizure thresholds or performing MES or 6-Hz seizure, no anesthetics or analgesics were used, to reduce the possibility of a pharmacodynamic or pharmacokinetic interaction between these agents and the examined compounds. Each animal was used only once in acute seizure test. Following acute seizure tests, the surviving mice were euthanized by >70% carbon dioxide (CO_2) or by cervical dislocation by a person trained for this procedure.

Adult zebrafish (*Danio rerio*) stocks of AB strain (Zebrafish International Resource Center, Oregon, USA) were maintained at standard aquaculture conditions, i.e., 28.5˚C, on a 14/10 h light/dark cycle in 8.0 L tanks [27 cm long, 21 cm wide and 17 cm high]. Fertilized eggs were collected via natural spawning. Embryos were reared under constant light conditions in embryo medium, i.e., Danieu's buffer: 1.5 mM Hepes, pH 7.6, 17.4 mM NaCl, 0.21 mM KCI, 0.12 mM $MgSO_4$ and 0.18 mM $Ca(NO_3)_2$. All embryos and larvae were kept in incubator, at 28.5˚C. The maximum tolerated concentration was evaluated in n=144 larvae of 4 days post-fertilization (dpf). For EEG experiments, n=80 larvae of 6 dpf were used.

Maximal electroshock seizures

MES induced seizure is among the most widely used rodent models of acute seizure [23]. 1% ophtalmic solution of tetracaine was administered for a short-term topical ophthalmic aneasthesia. Then, constant current stimuli (sine-wave pulses at 50 Hz for 200 ms) were applied via saline-soaked transcorneal electrodes with the usage of rodent shocker (type 221; Hugo Sachs Elektronik, Freiburg, Germany). During stimulation, mice were restrained manually and immediately following stimulation they were placed in a transparent box without bedding for behavioral observation on the presence or absence of seizure activity. Tonic hindlimb extension, defined as the rigid extension of the hindlimb that exceeds a 90° angle with the body, was considered as an endpoint.

Two experimental approaches were used: (1) the MEST test that employed stimulation at varied current intensities (7.6–17.4 mA) and (2) MES that employed stimulation at a fixed current intensity (50 mA). The mice were injected with a single dose of TC-G 1008, $ZnCl_2$, VPA or VEH. 30 min later the MEST test was performed. The threshold current was established according to an 'up-and-down' method described by Kimball et al. [24]. Current intensity was lowered or raised by 0.06-log intervals depending on whether the previously

stimulated animal did or did not exert tonic hindlimb extension, respectively. The data obtained in groups of 20 animals were used to determine the threshold current causing endpoint in 50% of mice (CS_{50} with confidence limits for 95% probability). In the MEST test, the dose-response relationship was assessed. An initial dose of TC-G 1008 or $ZnCl_2$ was selected and the dose was either increased or decreased in a subsequent group of mice, depending on whether the previous dose affected the seizure threshold. The dose of VPA has been established to increase seizure threshold in this test [25]. Following MEST, the mice were euthanized by >70% carbon dioxide (CO_2).

Groups of mice (n=10) were injected with a single dose of TC-G 1008, $ZnCl_2$, VPA or VEH. 30 min later they were stimulated with supramaximal MES stimulus of 50 mA. The doses of drugs applied before MES were based on the results of the MEST test – either effective or ineffective doses of TC-G 1008 and $ZnCl_2$ were administered. Control, non-stimulated (sham) animals received the respective doses of drugs or VEH but did not receive MES stimulus.

Six hertz (6 Hz) seizures

The 6-Hz seizure model is another model of acute seizures which is required while screening for antiseizure drugs [26]. 1% ophtalmic solution of tetracaine was used for a short-term topical ophthalmic anaesthesia. Then, square-wave alternating current stimuli (0.2-ms duration pulses at 6 Hz for 3 s) were applied via corneal electrodes using a Grass model CCU1 constant current unit coupled to a Grass S48 stimulator (Grass Technologies, Warwick, RI, USA). Before stimulation, the corneal electrodes were wetted with saline to provide good electrical contact. Mice were manually restrained during stimulation. Immediately following the stimulation, mice were placed in a transparent box without bedding for behavioral observation. The 6-Hz seizures were characterized by stun (fixed) posture, rearing, forelimb

clonus, twitching of the vibrissae, and elevated tail. Lack of the features listed above or the resumption of normal exploratory behavior within 10 s after stimulation were considered as the absence of seizures.

Two experimental approaches were used: (1) the 6-Hz seizure threshold test that employed stimulation at varied current intensities (10.0–20.0 mA) and (2) the 6-Hz seizure which was induced by supramaximal stimulation at a fixed current intensity (32 mA). The mice were injected with a single dose of TC-G 1008, $ZnCl_2$, VPA or VEH. 30 min later the 6-Hz seizure threshold test was performed. The current intensity values were established according to an 'up-and-down' method [24]. The animals were stimulated at current intensity that was lowered or raised by 0.06-log intervals depending on whether the previously stimulated animal did or did not respond with seizures, respectively. The data obtained in groups of 20 animals were used to determine the threshold current causing 6-Hz-induced seizures in 50% of mice (CS_{50} with confidence limits for 95% probability). In the 6-Hz threshold test, the dose-response relationship was assessed. An initial dose of TC-G 1008 or $ZnCl_2$ was selected and the dose was either increased or decreased in a subsequent group of mice, depending on whether the previous dose affected the seizure threshold. The dose of VPA has been established to increase seizure threshold in this test [25]. Following the 6-Hz seizure threshold test, the mice were euthanized by >70% carbon dioxide (CO_2).

Groups of mice (n=8) were injected with a single dose of TC-G 1008, $ZnCl_2$ or VPA, which was effective in the 6-Hz threshold test, or VEH. 30 min later the mice were stimulated with supramaximal current intensity of 32 mA. Control, non-stimulated (sham) animals received the respective doses of drugs or VEH but did not receive the supramaximal current intensity of 32 mA.

Kainic acid-induced seizures

Groups of mice (n=8-12) were injected *i.p.* with a single dose of TC-G 1008, $ZnCl_2$ or VEH. 30 min later the mice were injected *i.p.* with a single dose of KA (40 mg/kg) [27]. Immediately following KA injection, mice were placed individually into a transparent box without bedding for 2 h for behavioral observation. Seizure severity of each mice was scored according to the modified Racine's scale: stage 0, no response; stage 1, immobility and staring; stage 2, scratching/myoclonic jerks; stage 3, forelimb clonus; stage 4, rearing; stage 5, rearing and falling; stage 6, jumping, circling, rolling; stage 7, status epilepticus, death [27-29]. The dose-response relationship was assessed. An initial dose of TC-G 1008 or $ZnCl_2$ was selected and the dose was either increased or decreased in a subsequent group of mice, depending on whether the previous dose exerted a response. The surviving animals were immediately euthanized by >70% carbon dioxide (CO_2).

Intravenous pentylenetetrazole (PTZ) seizures

PTZ induced seizure is among the most widely used rodent models of acute seizure [23]. Groups of mice (n=9-12) were injected *i.p.* with a single dose of TC-G 1008, $ZnCl_2$, VPA or VEH. 30 min later the mice were placed in the cylindrical plastic restrainer (12-cm long, 3-cm inner diameter). The lateral tail vein was catheterized with a 2-cm long 27-gauge needle attached by polyethylene tubing PE20RW (Plastics One Inc., Roanoke, VA, USA) to a 5-ml plastic syringe containing 1% aqueous solution of PTZ. The syringe was mounted on a syringe pump (model Physio 22, Hugo Sachs Elektronik–Harvard Apparatus GmbH, March-Hugstetten, Germany). The accuracy of needle placement in the vein was confirmed by appearance of blood in the tubing. The needle was secured to the tail by an adhesive tape. Following catheterization, mice were released from the restrainer and placed in a Plexiglas arena for behavioral observation. The PTZ solution was infused at a constant rate of 0.2

ml/min. The time intervals from the commencement of PTZ infusion to the onset of each of three endpoints (the first myoclonic twitch, generalized clonus with loss of the righting reflex, and tonic forelimb extension) were recorded. The PTZ infusion was stopped at the beginning of tonic seizures, which were usually lethal for mice. All surviving animals were euthanized immediately by cervical dislocation. The seizure thresholds were calculated separately for each endpoint using the following formula: threshold dose of PTZ (mg/kg) = (infusion duration (s) × infusion rate (ml/s) × PTZ concentration (mg/ml))/body weight (kg) and were expressed as the dose of PTZ (in mg/kg) needed to produce the first apparent sign of each endpoint. The dose-response relationship was assessed. An initial dose of TC-G 1008 or $ZnCl_2$ was selected and the dose was either increased or decreased in a subsequent group of mice, depending on whether the previous dose affected the seizure threshold. The dose of VPA has been established to increase seizure threshold in this test [25]. Data obtained in the *i.v.* PTZ seizure threshold test are presented as the amount of PTZ (in mg/kg) ± SEM needed to produce the first apparent sign of each endpoint in each experimental group.

PTZ kindling model

PTZ-kindling model in mice has been established as a model for epileptogenesis [30]. The mice were injected *i.p.* with VEH, TC-G 1008, $ZnCl_2$ or VPA on every alternate day. 30 min later, they were injected *i.p.* with a subthreshold dose of PTZ. The subthreshold doses of PTZ, which induce kindling phenomenon, range from 25 to 45 mg/kg [30]. In the case of kindling in Swiss Albino mice, the dose of PTZ was 40 mg/kg, as determined in our previous study [31]. In the case of kindling in C57BL/6/Tar x CBA/Tar mice, the dose of PTZ was 25 mg/kg, as determined in our preliminary experiment. Immediately following PTZ injection, mice were placed individually into a transparent box without bedding for 30 min for behavioral observation. Seizure severity of each subject was scored using the modified

Racine's scale: stage 0, no response; stage 1, immobility, ear and facial twitching; stage 2, myoclonic jerks; stage 3, forelimb clonus, stage 4, clonic seizure with rearing and falling; stage 5, generalized clonic seizure with loss of righting reflex; stage 6, tonic fore- and hindlimb extension [31]. The mean seizure severity scores were calculated for all experimental groups after each PTZ injection. Control, non-kindled animals received the respective doses of drugs but were injected with physiological saline instead of PTZ solution. PTZ kindling models were terminated to reduce potential mortality when any of the groups displayed consecutive stage 5 or 6 seizures. The group of Swiss Albino mice receiving TC-G 1008 and the WT group of C57BL/6/Tar x CBA/Tar mice receiving TC-G 1008 displayed the highest seizure score during respective PTZ kindling models. 15 Swiss Albino mice per group or 15 WT and 15 GPR39 KO mice were used in PTZ kindling models.

Grip-strength test

The effects of single doses of TC-G 1008, $ZnCl_2$ or VPA or repeated doses of these compounds and PTZ kindling on skeletal muscular strength were evaluated in Swiss Albino mice or C57BL/6/Tar x CBA/Tar mice using the grip-strength test [32]. The grip-strength apparatus (BioSeb, Chaville, France) consisted of a steel wire grid (8 × 8 cm) connected to an isometric force transducer. The animal was lifted by its tail so that it could grasp the grid with its forepaws. The mouse was then gently pulled backward until it released the grid and the maximal force in newtons (N) exerted by the mouse before losing grip was measured. The procedure was repeated three times and the mean force exerted by each mouse before losing grip was recorded. The mean force was then normalized to body weight and expressed in mN/g ± SE.

Chimney test

The effects of single doses of TC-G 1008, $ZnCl_2$ or VPA or repeated doses of these compounds and PTZ kindling on motor deficits were evaluated in Swiss Albino mice or C57BL/6/Tar x CBA/Tar mice using the chimney test [32]. In this test, the inability of animals to climb back-ward up through a Plexiglas tube (3 cm, inner diameter × 30 cm, length) within 60 s was an indicator of motor impairment.

Toxicological assessment in zebrafish

The maximum tolerated concentration was evaluated prior further experiments in zebrafish laravae. Groups (n=12) of 4 dpf zebrafish larvae were incubated with a range of TC-G 1008 or $ZnCl_2$ doses at 28.5˚C for 18 hours. 6 doses of each compound (TC-G 1008 or $ZnCl_2$) were tested. The following parameters were scored after 2 and 18 h of exposure: touch response, posture, edema, morphology, signs of necrosis, swim bladder and heartbeat. The dose of 65 µM Zn and 70 µM TC-G 1008 were chosen for EEG experiments.

EEG discharges assessment in zebrafish

PTZ-induced acute seizure model in zebrafish larvae is well-validated in terms of predictive validity and allows one to assess EEGs [33, 33, 34]. A single 6 dpf zebrafish larvae were placed in a 48-well plate (one larva per well) filled with 200 µl of VEH, $ZnCl_2$ or TC-G 1008 solution. Subsequently, larvae were incubated for 20 h at 28.5˚C. After incubation, larvae were exposed to VEH or 20 mM PTZ for 5 min. Thereafter, larvae were immobilized in a thin layer of 2% low-melting-point agarose and the glass electrode (resistance 1-5 MΩ) filled with artificial cerebrospinal fluid (124 mM NaCl, 2 mM KCl, 2 mM $MgSO_4$, 2 Mm $CaCl_2$, 1.25 mM KH_2PO_4, 26 mM $NaHCO_3$, 10 mM glucose) was placed into the optic tectum (MultiClamp 700B amplifier, Digidata 1550 digitizer, Axon instruments, USA) [33, 35]. Single recordings for each larva were performed for a period of 20 minutes. The discharges

were analyzed according to the duration of spiking paroxysms and only those were taken into account when the amplitude exceeded three times the background noise. The data were analyzed with the aid of Clampfit 10.2 software (Molecular Devices Corporation, USA) and custom-written programme for R (Windows). For EEG discharges assessment, n=5-17 larvae per group were used.

Tissue processing for biochemical analysis

For LC-MS/MS analysis, the mice were killed by rapid decapitation at four time points (15, 30, 60 and 120 min) after *i.p.* injection of TC-G 1008. For Western blot, ZP-1 staining and ICP-OES analysis the mice were killed ca. 3 min after MES or 6-Hz seizure or 24 h after the completion of the kindling paradigm. The brains were rapidly dissected and immersed in cooled (2-8°C) 0.9% NaCl solution. For LC-MS/MS analysis, the whole brains were frozen. For Western blot and ZP-1 staining, the brains were rapidly dissected on a cold plate into left and right hemispheres. Left hippocampi (dorsal and ventral) were dissected, immediately frozen on dry ice and stored at -80°C until Western blot analysis. The right hemispheres were frozen by liquid nitrogen and were stored at −80°C until cryo-sectioning. The trunk blood was collected into tubes without anti-coagulant. The blood was allowed to clot for 15-20 min and then centrifuged for 10 min at 5600 rpm at 4°C. The resulting supernatant (serum) was pipetted into tubes that were stored at -80°C until LC-MS/MS or ICP-OES analysis. The biochemical analyses were performed by experimenters blinded for the treatment.

Determination of TC-G 1008 concentrations by LC-MS/MS

The concentrations of TC-G 1008 were determined in serum and brain of Swiss Albino mice 15, 30, 60 and 120 min after compound administration (20 mg/kg, *i.p.*), using the LC-MS/MS method. The brains were homogenized in distilled water (1:3, *w*/*v*) with a tissue

homogenizer TH220 (Omni International, Inc., Warrenton, VA, USA). Purification of the samples was performed by protein precipitation procedure with 0.1% formic acid in acetonitrile containing pentoxifylline used as an internal standard (2000 ng/mL) added to the samples at the ratio of 1:2 (*v/v*). Then, the samples were shaken for 10 min (IKA Vibrax VXR, Germany) and after centrifugation (Minispin, Eppendorf, Germany) for 10 min at the 12 000 rpm the supernatant was transferred into autosampler vials. The HPLC system (Agilent 1100, Agilent Technologies, Waldbronn, Germany) consisted of a degasser, binary pump, column oven and an autosampler. Chromatographic separation was carried out on an XBridge™ C18 analytical column (3x50 mm, 5µm, Waters, Ireland) with the oven temperature set at 30°C. The autosampler temperature was maintained at 10°C and a sample volume of 15 µL was injected into the LC-MS/MS system. The mobile phase containing 0.1% formic acid in acetonitrile (A) and 0.1% formic acid in water (B) was set at a flow rate of 0.4 mL/min. Initial mobile phase composition was 95% B with a linear gradient to 30% B in the first 5 min, then isocratic mode for 5 min with the subsequent rapid change back to 95% B in 0.1 min. The remaining time of elution was set at 95% B. The whole HPLC operation lasted 13 min. Mass spectrometric detection was performed on an Applied Biosystems MDS Sciex (Concord, Ontario, Canada) API 2000 triple quadrupole mass spectrometer equipped with an electrospray ionization (ESI) interface. ESI ionization in the positive ion mode was used for ion production. The tandem mass spectrometer was operated at unit resolution in the selected reaction monitoring mode (SRM), monitoring the transition of the protonated molecular ions *m/z* 419 to 305 and *m/z* 419 to 171 for compound TC-G 1008 (the first pair was used as a quantifier and the second pair was employed for the identity verification as a qualifier) and *m/z* 279 to 181 for the internal standard. The mass spectrometric conditions were optimized for TC-G 1008 by continuous infusion of the standard solution at the rate of 10 µL/min using a Harvard infusion pump. The ion source temperature was maintained at 400°C. The ionspray

voltage was set at 5500V. The curtain gas (CUR) was set at 20 psi and the collision gas (CAD) at 12 psi. The optimal collision energy (CE) was 45V. The following parameters of ion path were used as the most favorable ones: declustering potential (DP) at 31V, focusing potential (FP) at 340V and entrance potential (EP) at 6.5V. Data acquisition and processing were accomplished using the Applied Biosystems Analyst version 1.6 software. The calibration curves were constructed by plotting the ratio of the peak areas of TC-G 1008 to internal standard versus TC-G 1008 concentrations and generated by weighted (1/x) linear regression analysis. The validated quantitation ranges for this method were from 1 to 2000 ng/mL for serum and 3-1500 ng/g for brain tissue with accuracy from 89.88–110.13% and from 86.54–109.51% for serum and brain tissue, respectively. The assays were reproducible with low intra- and inter-day variation (coefficient of variation less than 15%). No significant matrix effect was observed and there were no stability related problems during the routine analysis of samples.

Western blot analysis

Hippocampi of Swiss Albino mice or C57BL/6/Tar x CBA/Tar mice were homogenized in 2% sodium dodecyl-sulfate solution (SDS) (BioShop Canada Inc), denatured at 95°C for 10 min and centrifuged at 10.000 RPM at 4°C for 5 min. The total protein concentration was quantified in the supernatant using a Pierce BCA Protein Assay Kit (Thermo Fisher Scientific, Pierce Biotechnology, Rockford, IL, USA). The samples containing 10 µg of protein were prepared using Novex® Tris-Glycine SDS Sample Buffer (Thermo Fisher Scientific, Carlsbad, CA, USA) and were resolved on a 4-15 % Mini-Protean TGX Precast gels (BIO-RAD Laboratories, Inc., USA). The molecular weight marker: Spectra Multicolor Broad Range Protein Ladder (Thermo Fisher Scientific Baltic, Vilnius, Lithuania) was used. The proteins were transferred on a nitrocellulose membrane (BIO-RAD

Laboratories, Inc., USA). The membranes were blocked for 60 min with 1% blocking reagent from the BM Chemiluminescence WB kit (Mouse/Rabbit) (Roche Diagnostic, Mannheim, Germany). The membranes were then incubated with mouse monoclonal antibody targeting phosphorylated CREB at Ser 133 (anti-phospho-CREB (Ser133) antibody, clone 10E9, Millipore Cat# 05-667, RRID:AB_309889, at a concentration of 0.5 µg/ml) or rabbit polyclonal antibody targeting BDNF (anti-BDNF antibody, Novus Cat# NB100-98682, RRID:AB_1290643, at a dilution of 1:1000), or rabbit polyclonal antibody targeting tyrosine-phosphorylated TrkB (anti-Trk B phosphorylated (pTyr 816) antibody, Novus Cat# NBP1-03499, RRID:AB_1522601, at a concentration of 10 µg/ml), or β-actin (β-actin antibody, mouse monoclonal clone AC-15, purified from hybridoma cell culture**,** Sigma-Aldrich Cat# A1978, RRID:AB_476692, at a concentration of 0.5 µg/ml**)** at 2-8°C overnight. The dilutions of primary antibodies were prepared using 0.5% blocking solution from the BM Chemiluminescence WB kit (Mouse/Rabbit). They were stored at 2-8°C and were reused up to two times. On the next day, after washing with TBST 3 x 10 min, the membranes were incubated for 30 min with horseradish peroxidase-linked (HRP-linked) secondary antibody from the BM Chemiluminescence WB kit (Mouse/Rabbit), or the anti-mouse IgG, HRP-linked, Cell Signaling Cat# 7076, RRID:AB_330924, at the dilution of 1:1000 (in case of β-actin) under constant shaking at room temperature (RT). The dilutions of secondary antibodies were always prepared fresh. After incubation with secondary antibodies, the membranes were washed with TBST 3 x 10 min. Secondary antibodies were detected using a BM Chemiluminescence WB kit (Mouse/Rabbit). The protein bands were visualized with the Fuji-LAS 4000 System. The density of each protein band was analyzed using imaging software (Fuji Image Gauge v 4.0) and was normalized by the optical density of the corresponding β-actin band.

Determination of total zinc concentration by ICP-OES

Serum samples of Swiss Albino mice or C57BL/6/Tar x CBA/Tar mice were defrosted. 200 µL of serum was transferred to digestion vessels (DigiTUBE SCP SCIENCE 50mL class A) and mixed with 1.5 mL of 65% Suprapur® nitric acid (Merck) and 5.0 mL of deionized water. Then vessels were placed in heating blocks (DigiPREP SCP SCIENCE) and were digested for 60 minutes at 120℃. After digestion vessels with solution were left to reach RT and filled with deionized water to 10 mL. The analysis was performed using PlasmaQuant PQ 9000 Analytik Jena AG. The following operating conditions of ICP-OES were used: power 13000 W, plasma gas 14.0 L/min, auxiliary gas 0.50 L/min, nebulizer gas 0.60 L/min, monitoring direction of the plasma flame was axial. Standard solution for calibration curves of zinc at the concentration of 200 µg/L was prepared by diluting zinc 1000 mg/L standard (PlasmaCAL SCP SCIENCE) with 0.5% nitric acid in deionized water. Analysis line used for zinc quantification was 206.2 nm.

Determination of intracellular zinc concentration by Zinpyr-1 staining

12 µm hippocampal coronal sections from Swiss Albino mice or C57BL/6/Tar x CBA/Tar mice were prepared using cryostat microtome Leica CM 1850, Germany. The sections were incubated with 4% paraformaldehyde solution with 4% sucrose in phosphate-buffered saline (PBS) at RT for 15 min and were rinsed with 0.01 M PBS solution. The sections were then incubated with a solution of a cell-membrane permeable fluorescent probe for zinc, ZP-1 (Santa Cruz Biotechnology, sc-213182) at the concentration of 5 µM for 1h at RT. The sections were double stained with 4',6-Diamidino-2-Phenylindole, Dihydrochloride (DAPI) (Sigma Aldrich, D9542) at the concentration of 300 nM. Additional sections were treated with membrane-permeable zinc chelator N,N,N',N'-Tetrakis(2-pyridylmethyl)ethylenediamine (TPEN) (Santa Cruz Biotechnology, sc-200131), at the

concentration of 10 μM, for 40 min, before staining with ZP-1 and DAPI [36]. The sections were imaged using Leica DM6000 B microscope. The low-magnification, grayscale images were analyzed for the mean ZP-1 intensities using Image J. The following regions of the hippocampus were chosen for the analysis: dentate gyrus (DG), CA1 and CA3 regions.

Data and statistical analysis

Data were analyzed using GraphPad Prism v. 5.03 (GraphPad Software, San Diego, CA, USA) or STATISTICA v. 13.3 (TIBCO Software Inc, Palo Alto, CA, USA). Acute seizure tests and grip-strength tests in Swiss Albino mice or C57BL/6/Tar x CBA/Tar mice were analyzed using unpaired Student's *t*-test or one-way analysis of variance (ANOVA) and the Dunnett's multiple comparison test. Kindling in Swiss mice was analyzed by the two-way ANOVA and the Dunnett's multiple comparison test. Kindling in C57BL/6/Tar x CBA/Tar mice was analyzed by the three-way ANOVA and the Bonferroni's multiple comparison test. The Fisher's exact probability test (https://www.graphpad.com/quickcalcs/contingency2) or the Chi-square test were employed to analyze the chimney test. Data obtained in zebrafish larvae were analyzed by the two-way ANOVA and the Bonferroni's multiple comparison test. For Western blot, ZP-1 staining and ICP-OES each sample was run in triplicate. These experiments were analyzed by the two-way ANOVA and the Bonferroni's multiple comparison test. All results are presented as the mean ± SEM. $p<0.05$ was considered statistically significant with 95% confidence. No statistical method was used to predetermine sample size. The sample size in each behavioral, EEG or biochemical experiment is shown in figure legends. Data were screened for outliers using the Grubbs's test (https://www.graphpad.com/quickcalcs/Grubbs1.cfm).

Results

TC-G 1008 is brain penetrant

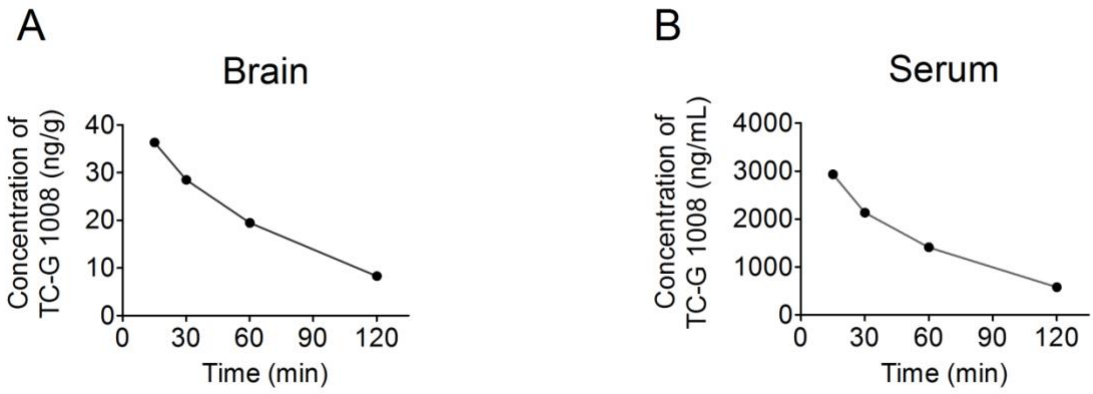

Fig 1. The concentrations of TC-G 1008 in the brain (**A**) and serum (**B**) of Swiss Albino mice over time following *i.p.* administration of a single dose of TC-G 1008 (20 mg/kg). N=4 in each group.

The concentration versus time profiles of TC-G 1008 in the brain and serum of Swiss Albino mice following *i.p.* administration of a single dose of TC-G 1008 (20 mg/kg) is shown in Fig 1. The mean concentration of TC-G 1008 in the brain was 36.32 ng/g 15 min after its *i.p.* administration at a dose of 20 mg/kg and 28.48 ng/g 30 min after dosing (Fig 1A). The molecular weight of TC-G 1008 is 481.9 Da. The estimated EC_{50} values are 0.4 and 0.8 nM for rat and human receptors, respectively [21], which corresponds to 0.193 ng/mL and 0.385 ng/mL. These data suggest that the concentrations of TC-G 1008 attained in the brain after its *i.p.* administration at the dose of 20 mg/kg are sufficient to occupy the GPR39 receptor. The mean concentrations of TC-G 1008 in serum were 2930 ng/mL and 2135 ng/mL after 15 and 30 min, respectively (Fig 1B). The serum levels of the studied compound were close to those obtained following oral administration of TC-G 1008 to male C57/Bl6 mice [21]. For example, the dose-normalized concentration at 60 min was 0.071 in this study and 0.06 when the compound was given orally at the dose of 10 mg/kg [21]. These data indicate that bioavailability of TC-G 1008 is comparable after both routes of administration.

The pharmacokinetic parameters of TC-G 1008 following administration of the dose of 20 mg/kg *i.p.* in Swiss Albino mice estimated using the non-compartmental approach, are shown in Table S1. TC-G 1008 was relatively slowly eliminated from serum and brain as the terminal half-life was about 50 min and the mean residence time values were over 70 min. The volume of distribution was high and significantly exceeded mouse whole body water, thus indicating an extensive distribution of the studied compound to organs and tissues. However, the penetration to brain tissue was rather limited as the brain-to-serum AUC ratio was 0.014. Nevertheless, the TC-G 1008 concentrations in this organ were sufficient to exert pharmacological effects at GPR39, which prompted us to examine its behavioral effects.

TC-G 1008 and $ZnCl_2$ exert divergent effects in the MEST and 6-Hz seizure threshold tests

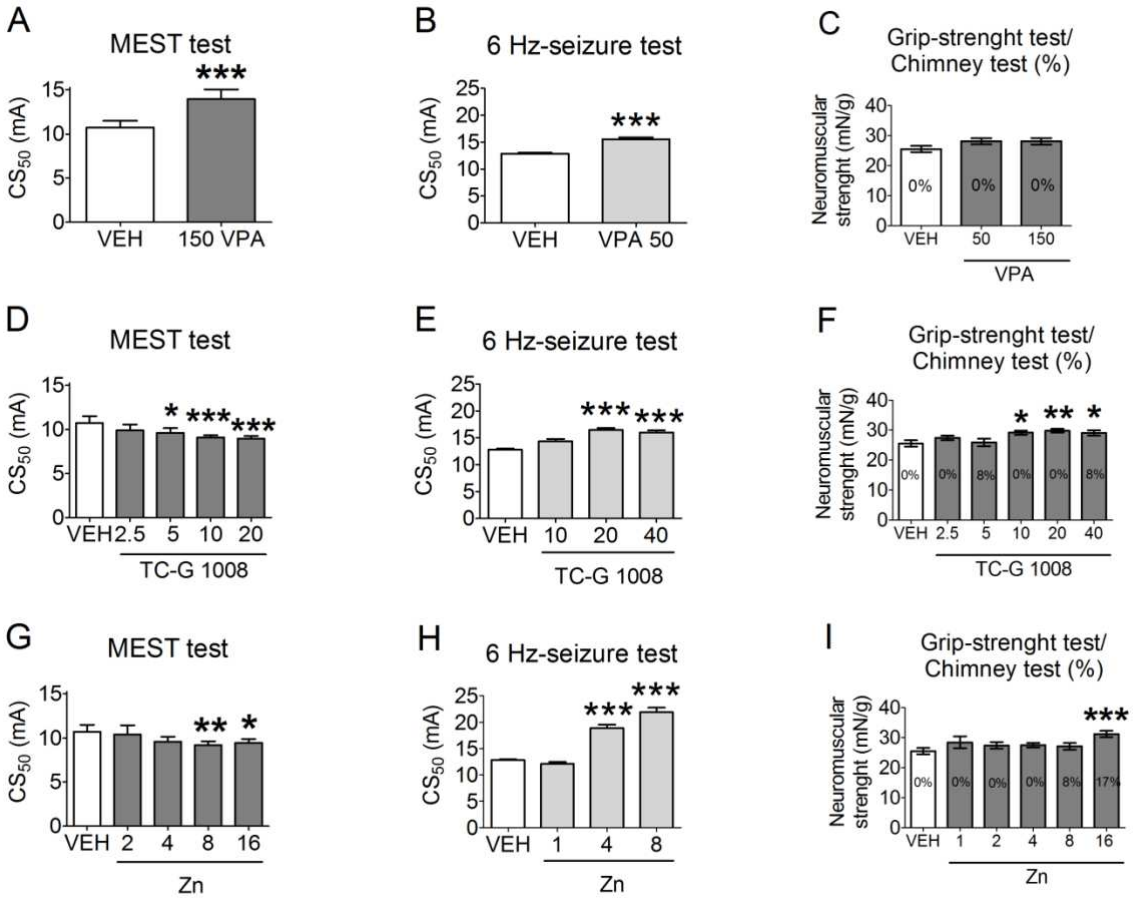

Fig 2. The effects of *i.p.* administration of single doses of VPA (**A, B, C**), TC-G 1008 (**D, E, F**) or $ZnCl_2$ (**G, H, I**) on the seizure threshold in the maximal electroshock seizure threshold (MEST) test (**A, D, G**), on the seizure threshold in the 6-Hz seizure threshold test (**B, E, H**), on neuromuscular strength in the grip-strength test and on motor coordination in the chimney test (**C, F, I**). The doses of compounds are shown on abscissas. Control animals received vehicle (VEH) (1% Tween 80 in 0.9% NaCl). Data from the MEST and 6-seizure threshold test were analyzed by the Student's t-test or one-way ANOVA and the Dunnett's multiple comparison test. They are presented as CS_{50} (in mA) values with upper 95% confidence limits. Data from the grip-strength test (expressed as means ± SEM of the neuromuscular strength) and the chimney test (expressed as % of animals which displayed impairment of motor coordination in this test) were analyzed by the one-way ANOVA and Dunnett's multiple comparison test or the Chi-square test, respectively. *P<0.05, **p<0.01, *** p<0.001 (by Student's t-test or Dunnett's multiple comparison test).

Statistical details:

(A) t(17)=5.037, p=0.0001, Student's t-test; n=20 in each group
(**B**) t(18)=4.336, p=0.0004, Student's t-test; n=20 in each group
(C) F(2,31)=2.03, p=0.1485**,** One-way ANOVA; n=12 VEH, n=12 VPA 150, n=10 VPA 50
(D) F(4,44)=7.202, p=0.0001, One-way ANOVA; n=20 in each group
(**E**) F(3,35)=9.292, p=0.0001, One-way ANOVA; n=20 in each group
(**F**) F(5,65)=3.924, p=0.0036, One-way ANOVA, n=12 in each group, outlier excluded in TC-G 1008 2.5 group; p=0.5331 Chi-square test, n=12 in each group
(G) F(4, 43)=4.080, p=0.0069, One-way ANOVA; n=20 in each group
(**H**) F(3, 31)=38.98, p<0.0001, One-way ANOVA; n=20 in each group
(**I**) F(5, 66)=2.381, p=0.0478, One-way ANOVA; p=0.1990 Chi-square test, n=12 in each group

TC-G 1008 and $ZnCl_2$, unlike VPA, decrease seizure threshold in the MEST test

The effects of TC-G 1008, $ZnCl_2$ or VPA in the MEST and 6-Hz seizure threshold tests are shown in Fig 2. TC-G 1008 at doses of 5, 10 and 20 mg/kg (Fig 2D) and $ZnCl_2$ at doses of 8 and 16 mg Zn/kg (Fig 2G) significantly decreased the threshold for tonic hindlimb extension in the MEST test. In contrast, the standard anti-seizure drug, VPA (150 mg/kg) significantly increased the threshold for seizure in this test (Fig 2A).

TC-G 1008 and $ZnCl_2$, as VPA, increase seizure threshold in the 6-Hz seizure threshold test

TC-G 1008 at doses of 20 and 40 mg/kg (Fig 2E) and $ZnCl_2$ at doses of 4 and 8 mg Zn/kg (Fig 2H) significantly increased the threshold for seizure in the 6-Hz seizure threshold test. Similarly, VPA (50 mg/kg) (Fig 2B) significantly increased the seizure threshold in this test.

In addition, TC-G 1008 at doses of 10, 20 and 40 mg/kg (Fig 2F) and $ZnCl_2$ a dose of 16 mg Zn/kg (Fig 2I) significantly increased the neuromuscular strength of mice in the grip-strength test. None of the administered compounds significantly impaired motor coordination of mice in the chimney test (Fig 2C, 2F, 2I).

The effects of acute treatment with TC-G 1008 and MES or 6-Hz seizures on $[Zn^{2+}]_I$ in the hippocampus and on total serum zinc

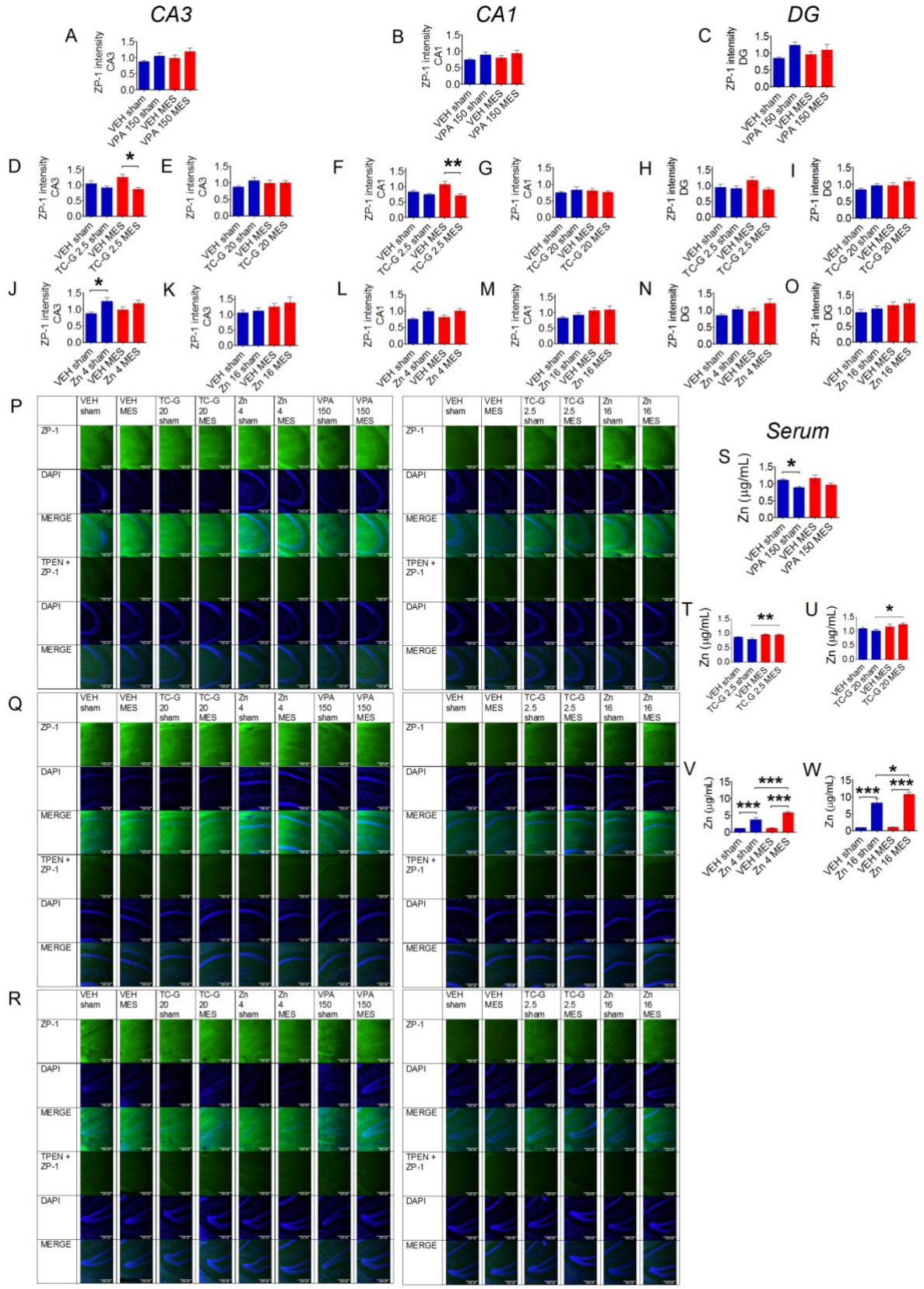

Fig 3. The effects of single doses of VPA, TC-G 1008 or $ZnCl_2$ and maximal electroshock seizure (MES), generated by supramaximal current intensity of 50 mA, on intracellular Zn^{2+} ($[Zn^{2+}]_I$) in the CA3, CA1 and dentate gyrus (DG) regions of the hippocampus (**A-O**) and on total serum zinc concentration (**S-W**). Drugs or VEH (1% Tween 80 in 0.9% NaCl) were administered *i.p.*, 30 min before MES, in Swiss Albino mice. Non-stimulated (sham) mice received the respective doses of drugs or VEH but they did not receive the electrical stimulus. Hippocampal sections from mice were double stained with Zinpyr-1 (ZP-1) for fluorescent-detection of $[Zn^{2+}]_I$ and with DAPI to show cell nuclei. The ratio of mean ZP-1 grey values between mouse sections belonging to treatment groups: VPA (**A-C**), TC-G 1008 (**D-I**) or $ZnCl_2$ (**J-O**) that received either MES or sham stimulation was analyzed at ca. 3 min after MES. Data were analyzed by the two-way ANOVA and a Bonferroni's multiple comparison test. *P<0.05, ** p<0.01 (by the Bonferroni's multiple comparison test). Magnification of ZP-1 (green), DAPI (blue) and TPEN / Zinpyr-1 in the CA3 (**P**), CA1 (**Q**) and DG (**R**) regions is shown. Merged images include ZP-1 (green) or TPEN / ZP-1 and DAPI (blue). ZP-1 fluorescence is mostly absent in TPEN-treated section, thus revealing the high specificity of the Zn^{2+}-staining in brain sections. Scale bar=200 μM. Total serum zinc concentration was measured by ICP-OES (**S-W**). Data were analyzed by the two-way ANOVA and the Bonferroni's multiple comparison test and are expressed as means ± SEM. *P<0.05, **p<0.01, ***p<0.001 (by the Bonferroni's multiple comparison test).

Statistical details:

(A) interaction [F(1,16)=0.03263, p=0.8589], VPA 150 [F(1,16)= 4.264, p=0.0555], MES [F(1,16)= 1.791, p=0.1995]; n=5 in each group

(B) interaction [F(1,16)=0.01224, p=0.9133], VPA 150 [F(1,16)=3.693, p=0.0726], MES [F(1,16)=0.4103, p=0.5309]; n=5 in each group

(C) interaction [F(1,15)=1.386, p=0.2574], VPA 150 [F(1,15)=5.565, p= 0.0323], MES [F(1,15)=0.01234, p=0.913]; n=5 in each group, sample loss in VPA 150 sham group, thus the analysis based on n=5 VEH sham, n=4 VPA 150 sham, n=5 VEH MES, n=5 VPA 150 MES

(D) interaction [F(1,16)=2.056, p=0.1708], TC-G 1008 2.5 [F(1,16)=9.034, p=0.0084], MES [F(1,16)= 0.7403, p=0.4023]; n=5 in each group

(E) interaction [F(1,16)=1.357, p=0.2612], TC-G 1008 20 [F(1,16)=1.668, p=0.2149], MES [F(1,16)=0.03546, p=0.853]; n=5 in each group

(F) interaction [F(1,16)=3.377, p=0.0848], TC-G 1008 2.5 [F(1,16)=9.198, p=0.0079], MES [F(1,16)=2.163, p=0.1607]; n=5 in each group

(G) interaction [F(1,16)=0.8636, p=0.3665], TC-G 1008 20 [F(1,16)=0.1068, p=0.748], MES [F(1,16)=0.005671, p=0.9409]; n=5 in each group

(**H**) interaction [F(1,16)=2.202, p=0.1573], TC-G 1008 2.5 [F(1,16)=3.424, p=0.0828], MES [F(1,16)=0.941, p=0.3465]; n=5 in each group

(I) interaction [F(1,16)=0.00189, p=0.9658], TC-G 1008 20 [F(1,16)=2.566, p=0.1288], MES [F(1,16)=2.295, p=0.1493]; n=5 in each group
(J) interaction [F(1,15)=0.7942, p=0.3869], Zn 4 [F(1,15)=8.5, p=0.0107], MES [F(1,15)= 0.04685, p=0.8316]; n=5 in each group, sample loss in Zn 4 MES group, thus the analysis based on n=5 VEH sham, n=5 Zn 4 sham, n=5 VEH MES, n=4 Zn 4 MES
(K) interaction [F(1,16)=0.04982, p=0.8262], Zn 16 [F(1,16)=0.5478, p=0.4699], MES [F(1,16)= 3.203, p=0.0925]; n=5 in each group
(L) interaction [F(1,15)=0.1167, p=0.7373], Zn 4 [F(1,15)=8.268, p=0.0116], MES [F(1,15)=0.1663, p=0.6892]; n=5 in each group, sample loss in Zn 4 MES group, thus the analysis based on n=5 VEH sham, n=5 Zn 4 sham, n=5 VEH MES, n=4 Zn 4 MES
(M) interaction [F(1,16)=0.1492, p=0.7044], Zn 16 [F(1,16)=0.3807, p=0.5459], MES [F(1,16)=4.087, p=0.0603]; n=5 in each group
(N) interaction [F(1,15)=0.07936, p=0.782], Zn 4 [F(1,15)= 4.254, p=0.0569], MES [F(1,15)=2.217, p=0.1572]; n=5 in each group, sample loss in Zn 4 sham group, thus the analysis based on n=5 VEH sham, n=4 Zn 4 sham, n=5 VEH MES, n=5 Zn 4 MES**(O)** interaction [F(1,16)=0.04564, p=0.8335], Zn 16 [F(1,16)=0.5955, p=0.4515], MES [F(1,16)= 2.996, p=0.1027; n=5 in each group
(S) interaction [F(1,35)=0.01585, p=0.9005], VPA 150 [F(1,35)=11.487, p=0.0018], MES [F(1,35)=1.154, p=0.29]; n=10 in each group, outlier excluded in VEH sham group, thus the analysis based on n=9 VEH sham, n=10 VPA 150 sham, n=10 VEH MES, n=10 VPA 150 MES
(T) interaction [F(1,29)=1.161, p=0.2902], TC-G 1008 2.5 [F(1,29)=1.743, p=0.1971], MES [F(1,29)=15.04, p=0.0006]; n=10 VEH sham, n=8 VEH MES, n=10 TC-G 1008 2.5 sham, n=7 TC-G 1008 2.5 MES, outliers excluded in VEH sham and TC-G 1008 2.5 sham groups, thus the analysis based on n=9 VEH sham, n=8 VEH MES, n=9 TC-G 1008 2.5 sham, n=7 TC-G 1008 2.5 MES
(U) interaction [F(1,35)=1.88, p=0.1791], TC-G 1008 20 [F(1,35)=0.0042637, p=0.9483], MES [F(1,35)=5.372, p=0.0264]; n=10 in each group, outlier excluded in VEH sham group, thus the analysis based on n=9 VEH sham, n=10 VEH MES, n=10 TC-G 1008 2.5 sham, n=10 TC-G 1008 2.5 MES
(V) interaction [F(1,35)=6.822, p=0.0132], Zn 4 [F(1,35)=80.05, p<0.0001], MES [F(1,35)=7.596, p=0.29]; n=10 in each group, outlier excluded in VEH sham group, thus the analysis based on n=9 VEH sham, n=10 VEH MES, n=10 Zn 4 sham, n=10 Zn 4 MES
(W) interaction [F(1,26)=2.696, p=0.1104], Zn 16 [F(1,35)=122.5, p<0.0001], MES [F(1,35)=3.097, p=0.088]; n=10 VEH sham, n=8 VEH MES, n=10 Zn 16 sham, n=9 Zn 16 MES, outlier excluded in VEH sham group, thus the analysis based on n=9 VEH sham, n=8 VEH MES, n=10 Zn 4 sham, n=9 Zn 16 MES
(A-T Two-way ANOVA)

The non-effective in the MEST test dose of TC-G 1008 decreases $[Zn^{2+}]_I$ in the hippocampus

The effects of TC-G 1008, $ZnCl_2$ or VPA and the supramaximal MES stimulus of 50 mA, on hippocampal $[Zn^{2+}]_I$ and total serum zinc concentration are shown in Fig 3. $[Zn^{2+}]_I$ was decreased in the CA3 (Fig 3D) and CA1 (Fig 3F) regions of the hippocampus of mice that received TC-G 1008 (2.5 mg/kg) and MES, compared to mice that received VEH and MES. There was a tendency towards decreased $[Zn^{2+}]_I$ also in the DG of these mice (Fig 3H). There were tendencies towards increased $[Zn^{2+}]_I$ in the CA3, CA1 and DG regions of the hippocampus after administration of VPA (150 mg/kg) in sham mice (Fig 3A, B, C). $[Zn^{2+}]_I$ was increased in the CA3 region of the hippocampus after administration of $ZnCl_2$ (4 mg Zn/kg) in sham mice (Fig 4J). There were tendencies towards increased $[Zn^{2+}]_I$ in the CA1 (Fig 3L) and DG (Fig 3N) after administration of 4 mg Zn/kg in sham mice. There were tendencies towards increased $[Zn^{2+}]_I$ in the CA3 (Fig 3K), CA1 (Fig 3M) and DG (Fig 3O) after administration of $ZnCl_2$ (16 mg Zn/kg) in sham mice. There were tendencies towards increased $[Zn^{2+}]_I$ in the CA3, CA1 and DG after administration of $ZnCl_2$ (4 or 16 mg Zn/kg) in mice that received MES (Fig 3 J-O).

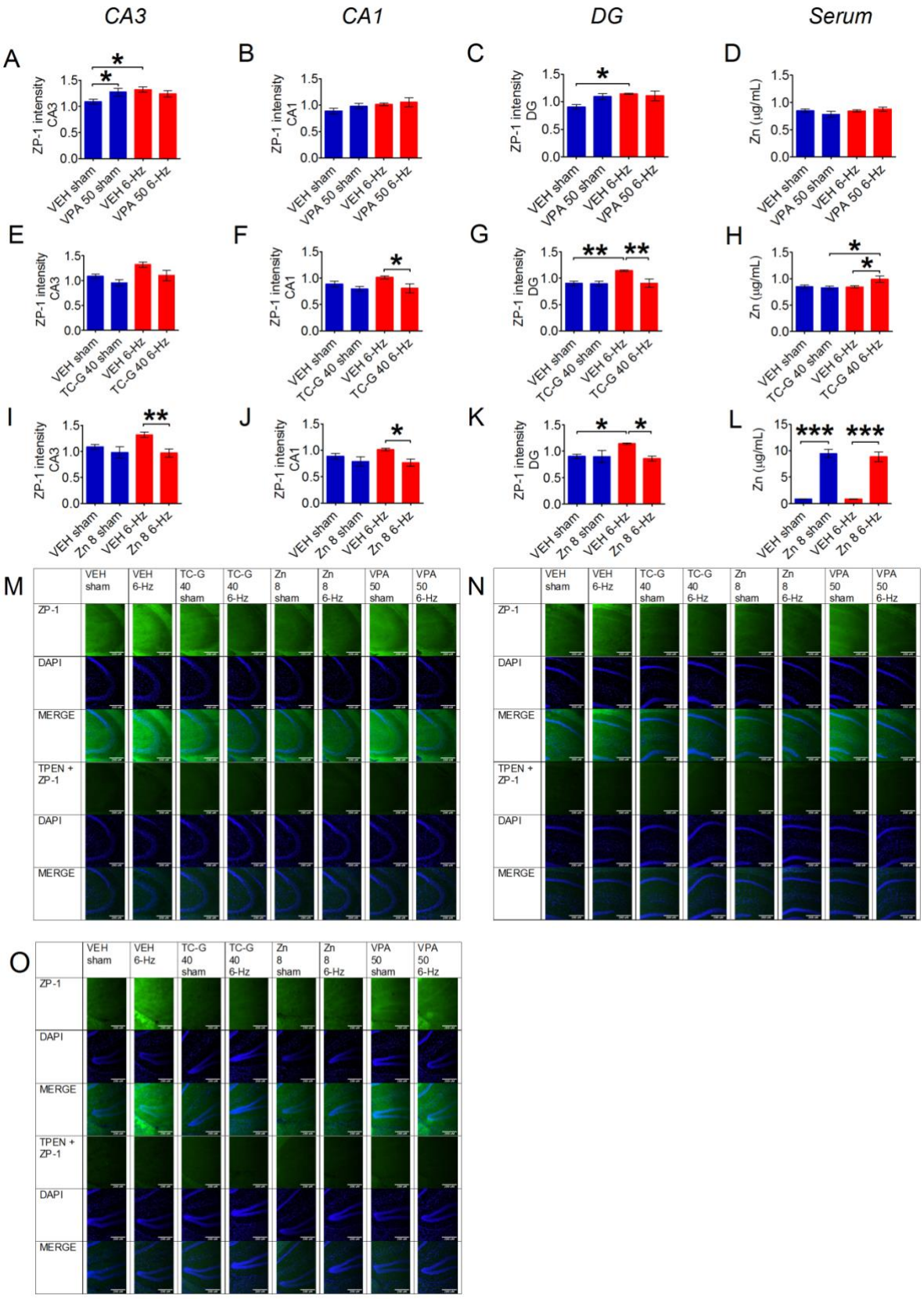

Fig 4. The effects of single doses of VPA, TC-G 1008 or $ZnCl_2$ and 6-Hz seizure, generated by supramaximal current intensity of 32 mA, on $[Zn^{2+}]_I$ in the CA3, CA1 and DG regions of the hippocampus (**A, E, I, B, F, J, C, G, K**) and on total serum zinc concentration (**D, H, L**).

Drugs or VEH (1% Tween 80 in 0.9 %NaCl) were administered *i.p.*, 30 min before 6-Hz seizure, in Swiss Albino mice. Non-stimulated (sham) mice received the respective doses of drugs or VEH but they did not receive the electrical stimulus. The ratio of mean ZP-1 grey values between mouse sections belonging to treatment groups: VPA (**A-C**), TC-G 1008 (**E-G**) or $ZnCl_2$ (**I-K**) that received either 6-Hz seizure or sham stimulation was analyzed at ca. 3 min after MES. Data were analyzed by the two-way ANOVA and a Bonferroni's multiple comparison test. *P<0.05, ** p<0.01 (by the Bonferroni's multiple comparison test). Magnification of ZP-1 (green), DAPI (blue) and TPEN / ZP-1 in the CA3 (**M**), CA1 (**N**) and DG (**O**) regions is shown. Merged images include ZP-1 (green) or TPEN / ZP-1 and DAPI (blue). ZP-1 fluorescence is mostly absent in TPEN-treated section, thus revealing the high specificity of the Zn^{2+}-staining in brain sections. Scale bar=200 μM. Total serum zinc concentrations were measured by ICP-OES (**D, H, L**). Data were analyzed by the two-way ANOVA and the Bonferroni's multiple comparison test and are expressed as means ± SEM. *P<0.05, ***p<0.001 (by the Bonferroni's multiple comparison test).

Statistical details:

(A) interaction [F(1,16)=5.22, p=0.0363], VPA 50 [F(1,16)=0.8289, p=0.3761], 6-Hz seizure [F(1,16)=2.951, p=0.1051]; n=5 in each group

(B) interaction [F(1,15)=0.2106, p=0.6525], VPA 50 [F(1,15)=1.317, p=0.268], 6-Hz seizure [F(1,15)= 2.944, p=0.1055]; n=5 in each group

(C) interaction [F(1,16)=4.193, p=0.0574], VPA 50 [F(1,16)=1.944, p=0.1823], 6-Hz seizure [F(1,16)= 5.297, p=0.0351]; n=5 in each group

(D) interaction [F(1,28)=1.627, p=0.2125], VPA 50 [F(1,28)=0.1678, p=0.6852], 6-Hz [F(1,28)=1.459, p=0.2371]; n=8 in each group

(E) interaction [F(1,15)=0.3827, p=0.5454], TC-G 1008 40 [F(1,15)=6.265, p=0.0244], 6-Hz seizure [F(1,15)=7.222, p=0.0169]; n=5 in each group, sample loss in TC-G 1008 40 sham group, thus the analysis based on n=5 VEH sham, n=4 TC-G 1008 40 sham, n=5 VEH 6-Hz, n=5 TC-G 1008 40 6-Hz

(F) interaction [F(1,15)=4.833, p=0.044], TC-G 1008 40 [F(1,15)=5.488, p=0.0334], 6-Hz seizure [F(1,15)=5.798, p=0.0294]; n=5 in each group, sample loss in TC-G 1008 40 sham group, thus the analysis based on n=5 VEH sham, n=4 TC-G 1008 40 sham, n=5 VEH 6-Hz, n=5 TC-G 1008 40 6-Hz

(G) interaction [F(1,15)=4.833, p=0.044], TC-G 1008 40 [F(1,15)=5.488, p=0.0334], 6-Hz seizure [F(1,15)=5.798, p=0.0294]; n=5 in each group, sample loss in TC-G 1008 40 sham group, thus the analysis based on n=5 VEH sham, n=4 TC-G 1008 40 sham, n=5 VEH 6-Hz, n=5 TC-G 1008 40 6-Hz

(H) interaction [F(1,28)=4.684, p=0.0391], TC-G 1008 40 [F(1,28)=3.135, p=0.0875], 6-Hz [F(1,28)= 4.393, p=0.0452]; n=8 in each group

(I) interaction [F(1,15)=2.746, p=0.117], Zn 8 [F(1,15)=9.592, p=0.0069], 6-Hz seizure [F(1,15)=2.185, p=0.1588]; n=5 in each group

(J) interaction [F(1,16)=1.368, p=0.2593], Zn 8 [F(1,16)=7.664, p=0.0137], 6-Hz seizure [F(1,16)= 0.7221, p=0.408]; n=5 in each group

(K) interaction [F(1,15)=4.603, p=0.0476], Zn 8 [F(1,15)=4.823, p=0.0432], 6-Hz seizure [F(1,15)=2.347, p=0.1451]; n=5 in each group

(L) interaction [F(1,28)=0.2557, p=0.617], Zn 8 [F(1,28)=189.2, p<0.0001], 6-Hz [F(1,28)= 0.2601, p=0.6141], n=8 in each group
(A-L Two-way ANOVA).

The seizure threshold-increasing in the 6-Hz seizure threshold test dose of TC-G 1008 decreases $[Zn^{2+}]_I$ in the hippocampus

The effects of TC-G 1008, $ZnCl_2$ or VPA and the 6-Hz seizure, generated by supramaximal current intensity of 32 mA, on hippocampal $[Zn^{2+}]_I$ and total serum zinc concentration are shown in Fig 4. Administration of VPA (50 mg/kg) increased $[Zn^{2+}]_I$ in the CA3 region of the hippocampus of sham mice (Fig 4A). The supramaximal current intensity of 32 mA increased $[Zn^{2+}]_I$ in the DG (Fig 4 C, G, K) region of the hippocampus. Administration of TC-G 1008 (40 mg/kg) and the supramaximal current intensity of 32 mA decreased $[Zn^{2+}]_I$ in the CA1 (Fig 4F) and DG (Fig 4G) regions of the hippocampus, compared to mice that received this stimulus and VEH. Similarly, administration of $ZnCl_2$ (8 mg Zn/kg) and the supramaximal current intensity of 32 mA decreased $[Zn^{2+}]_I$ in the CA3 (Fig 4I), CA1 (Fig 4J) and DG (Fig 4K) regions of the hippocampus, compared to mice that received this stimulus and VEH.

The acute effects of TC-G 1008 and MES or 6-Hz seizure on serum zinc concentration are not parallel to their effects on $[Zn^{2+}]_I$ in the hippocampus

Serum zinc concentration markedly and significantly increased after administration of single doses of $ZnCl_2$ of 4 mg Zn/kg (Fig 3V) or 16 mg Zn/kg (Fig 3W) in both sham mice and mice that received MES. Serum zinc concentration decreased after administration of VPA (150 mg/kg) in sham mice (Fig 3S). In turn, serum zinc concentration increased in mice that received TC-G 1008 at a dose of 2.5 (Fig 3T) or 20 (Fig 3U) mg/kg or $ZnCl_2$ at a dose of 4 mg

Zn/kg (Fig 3V) or 16 mg Zn/kg (Fig 3W) and MES, compared to sham mice that received the respective doses of drugs.

Serum zinc concentration markedly and significantly increased after administration of a single dose of $ZnCl_2$ (8 mg Zn/kg) in both sham mice and mice that received the supramaximal current intensity of 32 mA (Fig 4L). Also, serum zinc level increased in mice that received TC-G 1008 (40 mg/kg) and supramaximal current intensity of 32 mA, compared to sham mice that received the respective drugs. Similarly, serum zinc concentration increased in mice that received TC-G 1008 (40 mg/kg) and supramaximal current intensity of 32 mA compared to mice that received VEH and such stimulus (Fig 4H).

The effects of acute treatment with TC-G 1008 and $ZnCl_2$ on kainic acid-induced seizures and in the i.v. PTZ seizure threshold test

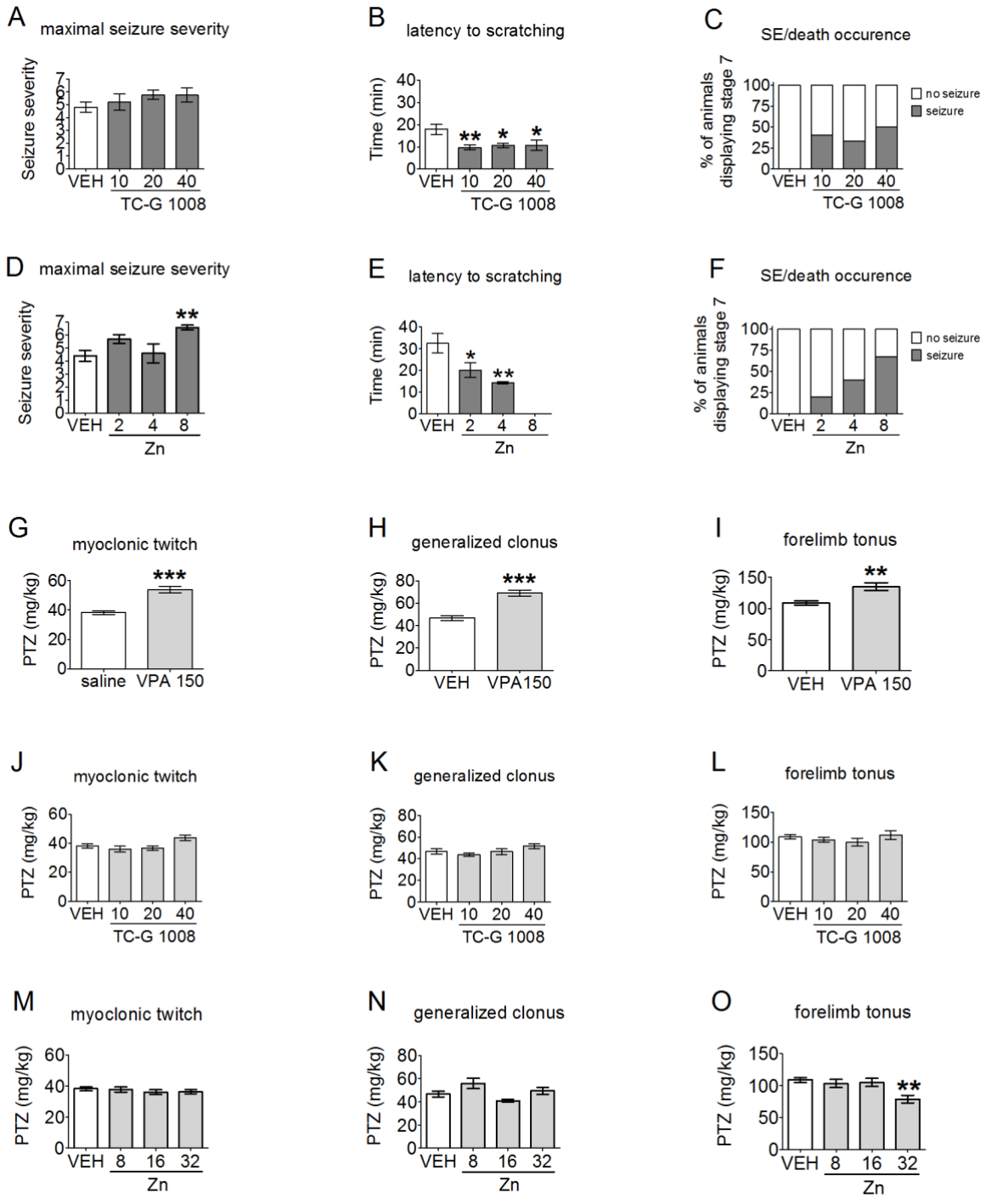

Fig 5. The effects of TC-G 1008 or $ZnCl_2$ on seizures induced by *i.p.* administration of kainic acid (KA) in Swiss Albino mice (**A-F**). The effects of VPA, TC-G 1008 or $ZnCl_2$ on seizures induced by *i.v.* infusion of pentylenetetrazole (PTZ) in Swiss Albino mice (**G-O**). TC-G 1008 (**A, B, C**) or $ZnCl_2$ (**D, E, F**) (the doses shown on abscissas) were administered *i.p.*, 30 min

before KA (40 mg/kg, *i.p.*) treatment in Swiss Albino mice. Control animals received vehicle (VEH) (1% Tween 80 in 0.9 %NaCl). Data were analyzed by the one-way ANOVA and Dunnett's multiple comparison test and are expressed as mean ± SEM. **P<0.01, *p<0.05 (the Dunnett's multiple comparison test). VPA (**G, H, I**), TC-G 1008 (**J, K, L**) or $ZnCl_2$ (**M, N, O**) (the doses shown on abscissas) were administered *i.p.*, 30 min before the *i.v.* infusion of PTZ in Swiss Albino mice. Control animals received vehicle (VEH) (1% Tween 80 in 0.9% NaCl). Data are presented as the dose of PTZ (in mg/kg) ± SEM needed to produce the first apparent sign of each endpoint. Data were analyzed by the Student's t-test or one-way ANOVA and Dunnett's multiple comparison test. ***P<0.001, **p<0.01 (the Dunnett's multiple comparison test).

Statistical details:

(A) F(3, 36)=0.8683, p=0.4673 (one-way ANOVA); n=10 VEH, n=10 TC-G 1008 10, n=10 TC-G 1008 20, n=8 TC-G 1008 40; outlier excluded in TC-G 1008 20 group, thus the analysis based on n=10 VEH, n=10 TC-G 1008 10, n=9 TC-G 1008 20, n=8 TC-G 1008 40

(B) F(3, 24)=5.549, p=0.0029 (one-way ANOVA), latency to scratching was not possible to measure in all mice because some of them proceeded immediately to advanced seizure stages. Therefore, n=10 VEH, n=9 TC-G 1008 10, n=7 TC-G 1008 20, n=6 TC-G 1008 40. 1 outlier was identified in each group and excluded, thus the analysis based on n=9 VEH, n=8 TC-G 1008 10, n=6 TC-G 1008 20, n=5 TC-G 1008 40

(C) Chi-square test, p=0.0951; n=10 VEH, n=10 TC-G 1008 10, n=10 TC-G 1008 20, n=8 TC-G 1008 40

(D) F(3, 38)=5.549, p=0.0029 (one-way ANOVA); n=10 VEH, n=10 Zn 2, n=10 Zn 4, n=12 Zn 8

(E) F(2, 20)=7.01, p=0.0049 (one-way ANOVA), latency to scratching was not possible to measure in all mice because some of them proceeded immediately to advanced seizure stages. Therefore, n=9 VEH, n=7 Zn 2, n=7 Zn 4. Mice that received 8 mg Zn/kg and KA proceeded immediately to advanced seizure stages

(F) Chi-square test, p=0.0074**;** n=10 VEH, n=10 Zn 2, n=10 Zn 4, n=12 Zn 8

(G) t(20)=6.395, p<0.0001 (the Student's t-test); n=12 VEH, n=10 VPA 150

(H) t(19)=6.235, p<0.0001 (the Student's t-test); n=12 VEH, n=9 VPA 150

(I) t(19)=3.689, p=0.0016 (the Student's t-test); n=12 VEH, n=9 VPA 150

(J) F(3, 37)=4.022, p=0.0142 (one-way ANOVA); n=12 VEH, n=10 TC-G 1008 10, n=10 TC-G 1008 20, n=9 TC-G 1008 40

(K) F(3, 35)=2.008, p=0.1308 (one-way ANOVA); n=12 VEH, n=10 TC-G 1008 10, n=9 TC-G 1008 20, n=9 TC-G 1008 40, outlier excluded in TC-G 20 group, thus the analysis based on n=12 VEH, n=10 TC-G 1008 10, n=8 TC-G 1008 20, n=9 TC-G 1008 40

(L) F(3, 34)=0.9246, p=0.4394 (one-way ANOVA); n=12 VEH, n=9 TC-G 1008 10, n=8 TC-G 1008 20, n=9 TC-G 1008 40

(M) F(3, 40)=0.5076, p=0.5076 (one-way ANOVA); n=12 VEH, n=11 Zn 8, n=11 Zn 16, n=10 Zn 32

(N) F(3, 37)=3.787, p=0.0182 (one-way ANOVA); n=12 VEH, n=10 Zn 8, n=9 Zn 16, n=11 Zn 32
(O) F(3, 38)=5.253, p=0.0039 (one-way ANOVA); n=12 VEH, n=10 Zn 8, n=11 Zn 16, n=9 Zn 32

$ZnCl_2$ increases maximal seizure severity in response to kainic acid

$ZnCl_2$ at a dose of 8 mg Zn/kg significantly increased the maximal seizure score in response to KA (40 mg/kg) (Fig 5D). Moreover, TC-G 1008 at doses of 10, 20 and 40 mg/kg (Fig 5B) and $ZnCl_2$ at doses of 2 and 4 mg Zn/kg (Fig 5E) significantly decreased the latency to scratching. This parameter was not possible to measure after administration of the dose of 8 mg Zn/kg because mice proceeded immediately to advanced seizure stages. The incidence of SE/ death (stage 7 seizure) was 40%, 33% and 50% after administration of TC-G 1008 at doses of 10, 20 and 40 mg/kg and KA (40 mg/kg), respectively (Chi-square test, $p>0.05$) (Fig 5C). In the case of $ZnCl_2$, the incidence of SE/ death was 20%, 40% and 67% following 2, 4 and 8 mg Zn/kg and KA (40 mg/kg), respectively (Chi-square test, $p<0.05$) (Fig 5F). Thus, $ZnCl_2$ significantly increased the incidence of SE/ death in response to KA. None of control mice injected with KA (40 mg/kg) exhibited SE/death.

$ZnCl_2$ decreases the threshold for forelimb tonus in the i.v. PTZ seizure threshold test

TC-G 1008 at doses of 10, 20 and 40 mg/kg (Fig 5J) and $ZnCl_2$ at doses of 8, 16 and 32 mg Zn/kg (Fig 5M) did not statistically significantly affect the threshold for myoclonic twitch. Also, these compounds did not statistically significantly affect the generalized clonus in this test (Fig 5H, K, N). TC-G 1008 at doses of 10, 20 and 40 mg/kg (Fig 5L) and $ZnCl_2$ at doses of 8 and 16 mg Zn/kg did not significantly affect the threshold for forelimb tonus while $ZnCl_2$ at a dose of 32 mg Zn/kg significantly decreased the threshold for this endpoint in this test (Fig 5O). VPA (150 mg/kg) significantly increased the seizure threshold for myoclonic twitch (Fig 5G), generalized clonus (Fig 5H) and forelimb tonus (Fig 5I).

The effects of TC-G 1008 on acute PTZ-induced seizures in zebrafish larvae and in chronic PTZ-induced kindling model of epilepsy in Swiss Albino mice

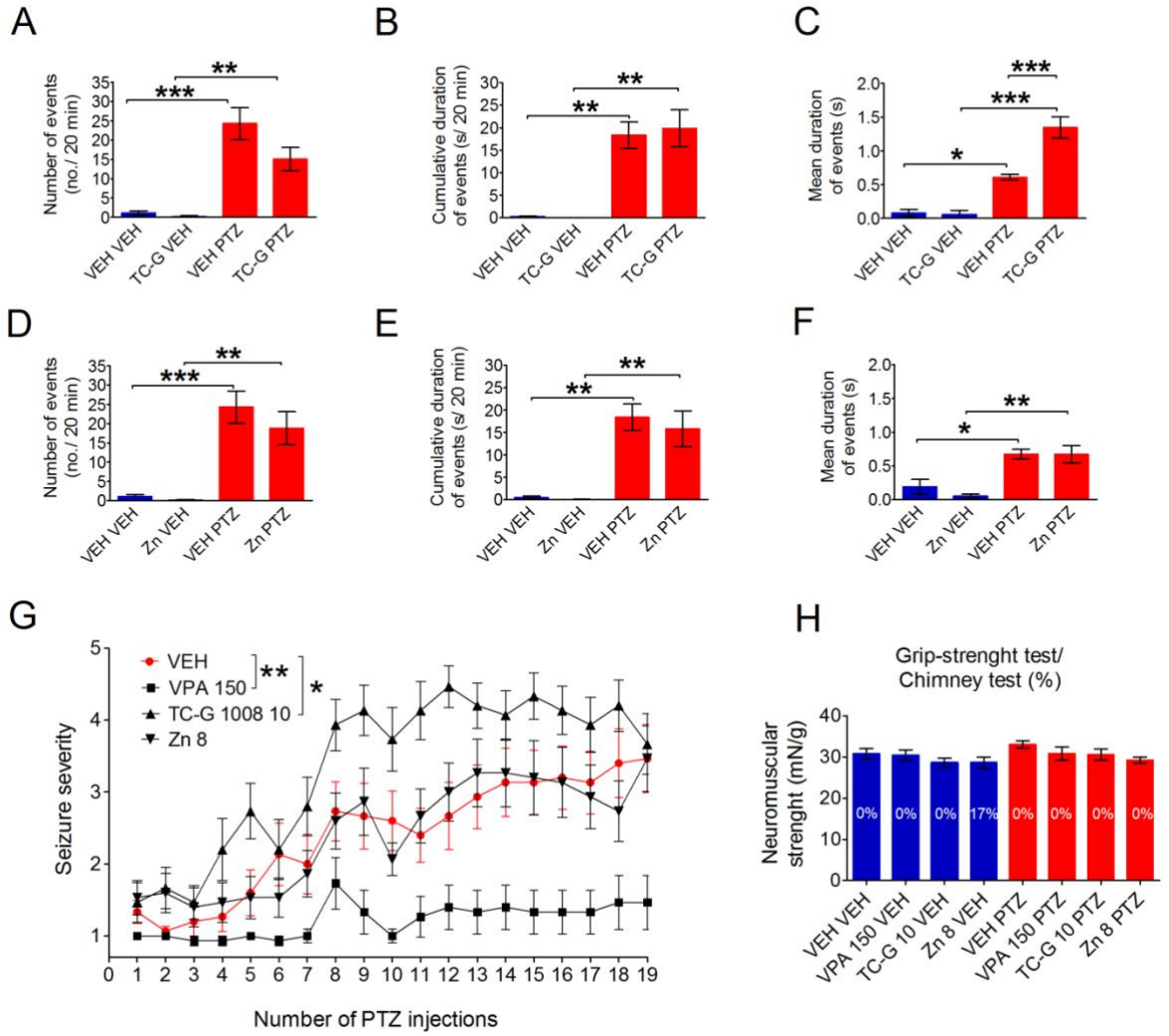

Fig 6. Electrophysiological recordings from the optic tectum of zebrafish larvae exposed to TC-G 1008 or $ZnCl_2$ and PTZ. Zebrafish larvae were incubated with VEH, TC-G 1008 (70 µM) or $ZnCl_2$ (65 µM) for 20 h, and subsequently exposed to VEH or PTZ (20 mM) for 5 min. The EEG recordings began 5 min after the removal of larva from VEH/PTZ solution and lasted 20 min. Results are expressed as means ± SEM of the number of epileptiform-like events, the cumulative duration of epileptiform-like events, and the mean duration of epileptiform-like events during 20 min of recordings. Data were analyzed using a two-way ANOVA and the Bonferroni's multiple comparison test. *P<0.05, **p<0.01, ***p<0.001 (by the Bonferroni's multiple comparison test) (**A-F**). The effects of chronic treatment with VPA, TC-G 1008 or $ZnCl_2$ on the development of PTZ kindling in Swiss Albino mice. VPA (150

mg/kg), TC-G 1008 (10 mg/kg), $ZnCl_2$ (8 mg Zn/kg) or VEH (1% Tween 80 in 0.9% NaCl) were injected *i.p.* once daily on every alternate day during weekdays. 30 min later, PTZ (40 mg/kg) was injected *i.p.* The total number of PTZ injections was 19. Data are expressed as means ± SEM of seizure severity and were analyzed by repeated measures ANOVA and a Dunnett's multiple comparison test. *P<0.05, **p<0.01 (by the Dunnett's multiple comparison test) (**G**). The effects of chronic treatment with VPA, TC-G 1008 or $ZnCl_2$ and PTZ kindling on neuromuscular strength in the grip-strength test and motor coordination in the chimney test in Swiss Albino mice. The non-kindled mice received the respective doses of drugs: VPA (150 mg/kg), TC-G 1008 (10 mg/kg), $ZnCl_2$ (8 mg Zn/kg) or VEH (1% Tween 80 in 0.9% NaCl) but received VEH instead of PTZ. The neuromuscular strength and motor coordination were assessed in kindled and non-kindled mice on the last day of PTZ kindling. Data from the grip-strength test (expressed as means ± SEM of the neuromuscular strength) and chimney test (expressed as % of animals which displayed impairment of motor coordination in this test) were analyzed by the two-way ANOVA or the Fisher's exact test, respectively (**H**).

Statistical details:

(A): interaction [F(1,33)=1.702, p=0.2011], TC-G 1008 [F(1,33)=2.522, p=0.1218], PTZ [F(1,33)=35.88, p<0.0001]; n=10 VEH VEH, n=8 VEH PTZ, n=5 TC-G 1008 VEH, n=14 TC-G 1008 PTZ

(B): interaction [F(1,31)=0.04892, p=0.8264], TC-G 1008 [F(1,31)=0.02596, p=0.8264], PTZ [F(1,31)=22.88, p<0.0001]; n=10 VEH VEH, n=8 VEH PTZ, n=5 TC-G 1008 VEH, n=14 TC-G 1008 PTZ, outliers excluded in VEH VEH and TC-G 1008 VEH groups, thus the analysis based on n=9 VEH VEH, n=8 VEH PTZ, n=4 TC-G 1008 VEH, n=14 TC-G 1008 PTZ

(C): interaction [F(1,30)=5.965, p=0.0207], TC-G 1008 [F(1,30)=5.385, p=0.0273], PTZ [F(1,30)=34.79, p<0.0001]; n=10 VEH VEH, n=8 VEH PTZ, n=5 TC-G 1008 VEH, n=14 TC-G 1008 PTZ, outliers excluded in VEH VEH and VEH PTZ groups, thus the analysis based on n=9 VEH VEH, n=7 VEH PTZ, n=5 TC-G 1008 VEH, n=14 TC-G 1008 PTZ

(D): interaction [F(1,38)=0.2952, p=0.5901], $ZnCl_2$ [F(1,38)=0.6019, p=0.4427], PTZ [F(1,38)=25.81, p<0.0001]; n=10 VEH VEH, n=8 VEH PTZ, n=8 $ZnCl_2$ VEH, n=17 $ZnCl_2$ PTZ, outlier excluded in Zn VEH group, thus the analysis based on n=10 VEH VEH, n=8 VEH PTZ, n=7 $ZnCl_2$ VEH, n=17 $ZnCl_2$ PTZ

(E): interaction [F(1,37)=0.07757, p=0.7822], $ZnCl_2$ [F(1,37)=0.156, p=0.6951], PTZ [F(1,37)=20, p<0.0001]; n=10 VEH VEH, n=8 VEH PTZ, n=8 $ZnCl_2$ VEH, n=17 $ZnCl_2$ PTZ, outliers excluded in VEH VEH and Zn VEH groups, thus the analysis based on n=9 VEH VEH, n=8 VEH PTZ, n=7 $ZnCl_2$ VEH, n=17 $ZnCl_2$ PTZ

(F): interaction [F(1,38)=0.3154, p=0.5777], $ZnCl_2$ [F(1,38)=0.3433, p=0.5614], PTZ [F(1,38)=20, p<0.0001]; n=10 VEH VEH, n=8 VEH PTZ, n=8 $ZnCl_2$ VEH, n=17 $ZnCl_2$ PTZ,

outlier excluded in VEH VEH group, thus the analysis based on n=9 VEH VEH, n=8 VEH PTZ, n=8 $ZnCl_2$ VEH, n=17 $ZnCl_2$ PTZ
(**A-F** Two-way ANOVA)
(G) Drug x time interaction [F (54, 1008)=2.546; p<0.0001], time [F (3.291, 184.3)=25.80; p<0.0001], drug [F (3, 56)=13.38, p<0.0001]; Two-way repeated measures ANOVA, n=15 in each group
(H): interaction [F(3,88)=0.3337, p=0.801], drug [F(3,88)=0.3337, p=0.1042], PTZ [F(1,88)= 2.37, p=0.1272], Two-way ANOVA; p>0.05 the Fisher's exact test, n=12 in each group

TC-G 1008 increases the mean duration of epileptiform-like events in zebrafish larvae

The effects of TC-G 1008 or $ZnCl_2$ on epileptiform-like events induced by PTZ in zebrafish larvae are shown in Fig 6A-F. Exposure to PTZ (20 mM) significantly increased the number of events, the cumulative duration of events and the mean duration of epileptiform-like events in zebrafish larvae. TC-G 1008 (70 µM) increased the mean duration of epileptiform-like events in larvae exposed to PTZ, compared to VEH (Fig 6C) but it did not affect the number of events (Fig 6A) or the cumulative duration of events (Fig 6B). Administration of $ZnCl_2$ (65 µM) in larvae exposed to PTZ did not affect the mean duration of epileptiform-like events (Fig 6D), the number of events (Fig 6E) or the cumulative duration of events (Fig 6F), compared to VEH. Administration of TC-G 1008 (70 µM) or $ZnCl_2$ (65 µM) also did not affect the assessed parameters in larvae treated with VEH instead of PTZ (Fig 6A-F).

TC-G 1008 facilitates the development of PTZ kindling **in mice**

The effects of TC-G 1008, $ZnCl_2$ or VPA on PTZ kindling in Swiss Albino mice are shown in Fig 6G. Repeated measures ANOVA showed a significant interaction between drug and time [F (54, 1008)=2.546, p<0.0001] regarding seizure severity during PTZ kindling in Swiss Albino mice. There was also a significant effect of time [F (3.291, 184.3)=25.80, p<0.0001] and drug [F (3, 56)=13.38, p<0.0001]. The Dunnett's multiple comparison test

showed that TC-G 1008 (10 mg/kg) increased the seizure severity compared with VEH treated mice (p=0.024368), while VPA decreased the seizure severity (p=0.001964) compared with VEH treated mice. After 19 injections of PTZ, the % of fully kindled mice was 6.7% of mice treated with VPA (150 mg/kg), 53% of mice treated with VEH, 67% of mice treated with $ZnCl_2$ (8 mg Zn/kg) and 87% of mice treated with TC-G 1008 (10 mg/kg) (Fisher's exact test p=0.0142 in the case of VPA 150, p=0.7104 Zn 8, p=0.0352 TC-G 1008 10). To reduce possible mortality in mice treated with TC-G 1008 (10 mg/kg), exhibiting consecutive stage 5 seizures, kindling was terminated after 19 injections.

The effects of chronic treatment with TC-G 1008 and PTZ-kindling in Swiss Albino mice on $[Zn^{2+}]_I$ in the hippocampus and on total serum zinc

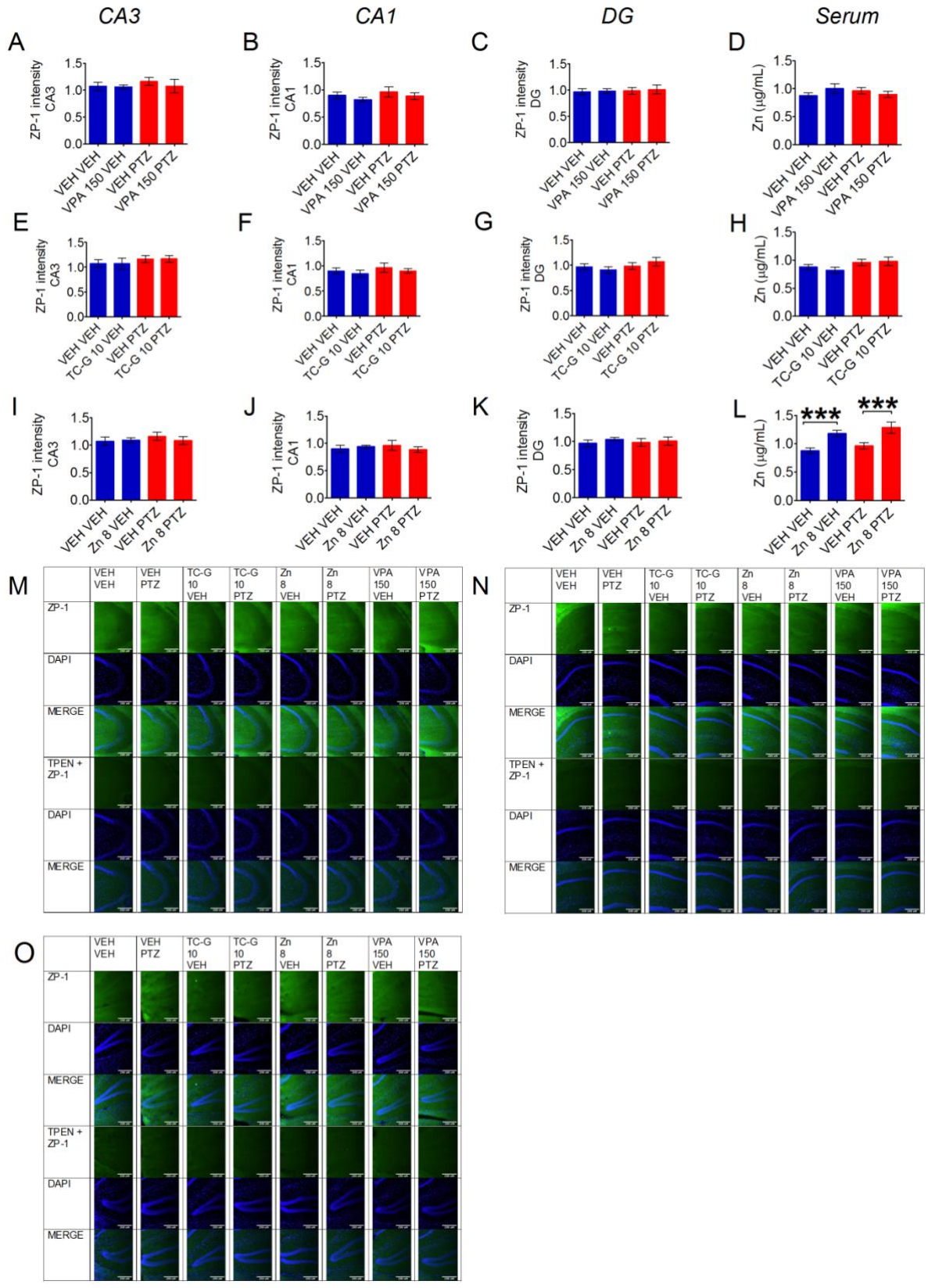

Fig 7. The effects of chronic treatment with VPA, TC-G 1008 or $ZnCl_2$ and PTZ kindling on $[Zn^{2+}]_I$ in the CA3, CA1 and DG regions of the hippocampus (**A, E, I, B, F, J, C, G, K**) and on total serum zinc concentration (**D, H, L**). VPA (150 mg/kg), TC-G 1008 (10 mg/kg), $ZnCl_2$ (8 mg Zn/kg) or VEH were injected *i.p.* once daily on every alternate day during weekdays. 30 min later, PTZ (40 mg/kg) was injected *i.p.* Non-kindled mice received the respective doses of drugs but received VEH instead of PTZ. The ratio of mean Zinpyr-1 grey values between mouse sections belonging to treatment groups: VPA (**A-C**), TC-G 1008 (**E-G**) or $ZnCl_2$ (**I-K**) that underwent PTZ kindling, which consisted of 19 injections, or of non-kindled, VEH-treated mice was measured at 24 h after the last injection of PTZ. Data were analyzed by the two-way ANOVA. Magnification of ZP-1 (green), DAPI (blue) and TPEN / ZP-1 in the CA3 (**M**), CA1 (**N**) and DG (**O**) regions is shown. Merged images include ZP-1 (green) or TPEN / ZP-1 and DAPI (blue). ZP-1 fluorescence is mostly absent in TPEN-treated section, thus revealing the high specificity of the Zn^{2+}-staining in brain sections. Scale bar=200 μM. Total serum zinc concentration was measured by ICP-OES (**D, H, L**). Data were analyzed by the two-way ANOVA and the Bonferroni's multiple comparison test and are expressed as means ± SEM. ***$p<0.001$ (by the Bonferroni's multiple comparison test).

Statistical details:

(A) interaction [F (1, 16)=0.1947, p=0.6649], VPA 150 [F (1, 16)=0.3107, p=0.850], PTZ kindling [F (1, 16)=0.4079, p=0.5321]; n=5 in each group

(B) interaction [F (1, 16)=0.000, p>0.9999], VPA 150 [F (1, 16)=1.378, p=0.2576], PTZ kindling [F (1, 16)=0.8626, p=0.3668]; n=5 in each group

(C) interaction [F (1, 16)=0.3412, p=0.5673], VPA 150 [F (1, 16)= .2439, p=0.6281], PTZ kindling [F (1, 16)=0.03236, p=0.8595]; n=5 in each group

(D) interaction [F(1,26)=3.134, p=0.0865], VPA 150 [F(1,26)=0.05726, p=0.8124], PTZ kindling [F(1,26)=3.134, p=0.0865]; n=10 in each group

(E) interaction [F (1, 16)=0.0006, p=00.9814], TC-G 1008 10 [F (1, 16)=0.0006, p=0.9814], PTZ kindling [F (1, 16)=1.265, p=0.2772]; n=5 in each group

(F) interaction [F (1, 16)=0.0051, p=0.9438], TC-G 1008 10 [F (1, 16)=0.6984, p=0.4156], PTZ kindling [F (1, 16)=0.6984, P=0.4156]; n=5 in each group

(G) interaction [F (1, 16)=2.037, p=0.1727], TC-G 1008 10 [F (1, 16)=0.1308, p=0.7224], PTZ kindling [F (1, 16)=0.4940, p=0.4923]; n=5 in each group

(H) interaction [F(1,27)=6.882, p=0.0144], TC-G 1008 10 [F(1,27)=8.387, p=0.0076], PTZ kindling [F(1,27)=10.65, p=0.0031]; n=10 in each group

(I) interaction [F (1, 16)=0.5715, p=0.4607], Zn 8 [F (1, 16)=0.1750, p=0.6813], PTZ kindling [F (1, 16)=0.3711, p=0.5510]; n=5 in each group

(J) interaction [F (1, 16)=0.0797, p=0.7814], Zn 8 [F (1, 16)=0.0078, p=0.9305], PTZ kindling [F (1, 16)=0.0006, p=0.9810]; n=5 in each group

(K) interaction [F (1, 16)=0.0289, p=0.8672], Zn 8 [F (1, 16)=0.8729, p=0.3640], PTZ kindling [F (1, 16)=0.4137, p=0.5292]; n=5 in each group

(L) interaction [F(1,27)=0.04264, p=0.8377], Zn 8 [F(1,27)=35.69, p<0.0001], PTZ kindling [F(1,27)=6.034, p=0.0195]; n=10 in each group
(A-L Two-way ANOVA).

Hippocampal $[Zn^{2+}]_I$ does not differ significantly after chronic treatment with TC-G 1008 in the PTZ-kindling model in Swiss Albino mice

There was a tendency towards increased [$Zn^{2+}]_I$ in the CA3 (Fig 7A, E, I) and CA1 (Fig 7B, F, J) regions of the hippocampus of mice subjected to PTZ-kindling model, which consisted of 19 injections of PTZ (40 mg/kg). There was a tendency towards decreased $[Zn^{2+}]_I$ in the CA1 region of the hippocampus of kindled-mice that received VPA (150 mg/kg) (Fig 7B), TC-G 1008 (10 mg/kg) (Fig 7F) or $ZnCl_2$ (8 mg Zn/kg) (Fig 7J), compared to kindled-mice that received VEH.

The effects of chronic treatment with TC-G 1008 on serum zinc concentration in the PTZ kindling model are not parallel to its effects on hippocampal $[Zn^{2+}]_I$

Serum zinc concentration increased after chronic treatment with $ZnCl_2$ (8 mg Zn/kg) in both kindled and non-kindled mice (Fig 7L). Such effect was not observed in either kindled or non-kindled mice after chronic treatment with TC-G 1008 (Fig 7H) or VPA (Fig 7D).

The effects of chronic treatment with TC-G 1008 and PTZ-kindling in Swiss Albino mice on hippocampal p-CREB, BDNF and p-TrkB proteins

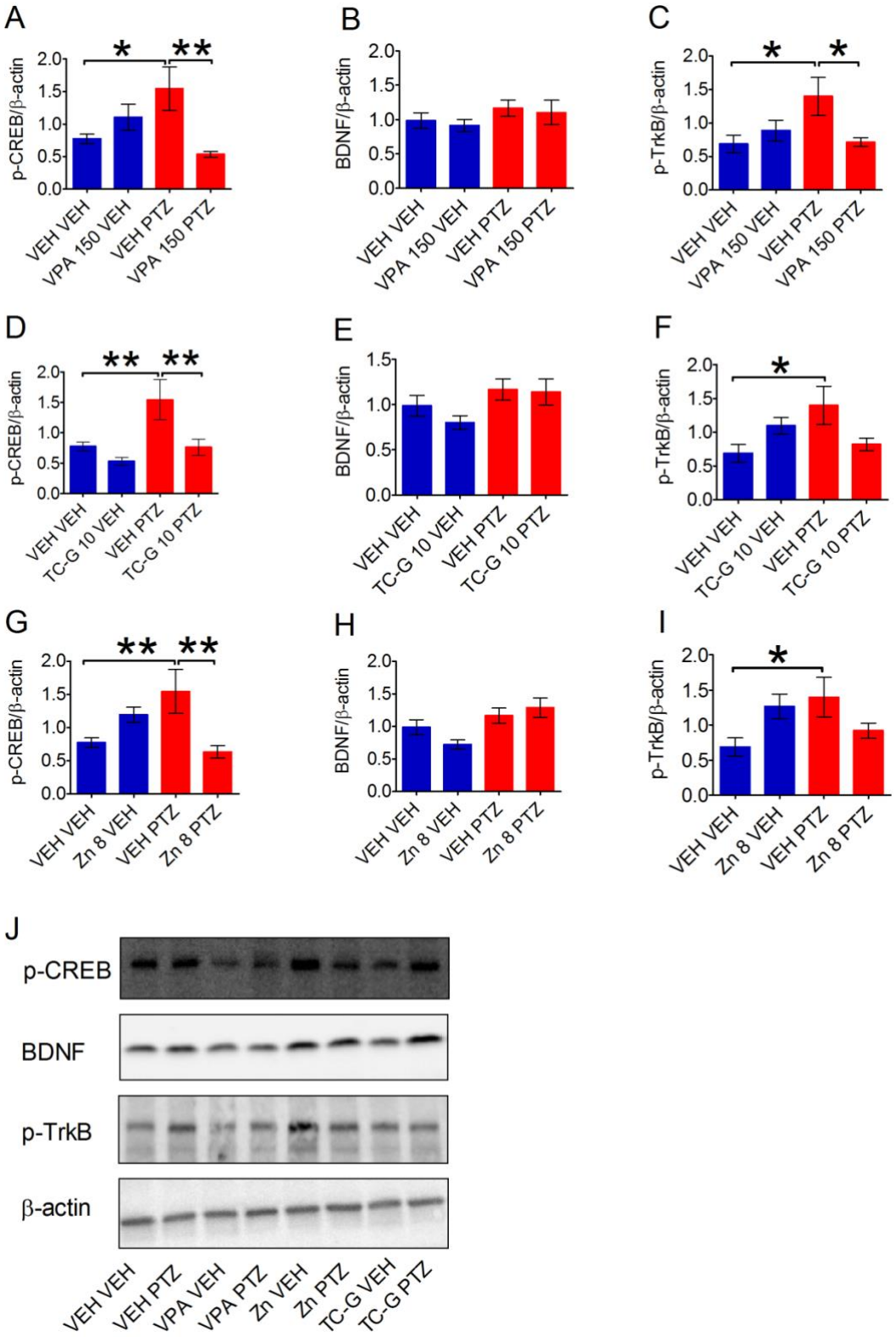

Fig 8. The effects of chronic treatment with VPA, TC-G 1008 or $ZnCl_2$ and PTZ kindling, which consisted of 19 injections of PTZ (40 mg/kg), on the relative expression of proteins: phosphorylated CREB at Ser 133 (p-CREB), BDNF or phosphorylated TrkB at Tyr 816 (p-TrkB) in the hippocampi of Swiss Albino mice at 24 h after the last PTZ injection. VPA (150 mg/kg), TC-G 1008 (10 mg/kg), $ZnCl_2$ (8 mg Zn/kg) or VEH (1% Tween 80 in 0.9% NaCl) were injected *i.p.* once daily on every alternate day during weekdays. 30 min later, PTZ (40 mg/kg) was injected *i.p.* Non-kindled mice received the respective doses of drugs but received VEH instead of PTZ. The results (mean ± SEM) are presented as the p-CREB or BDNF or p-TrkB/β-actin ratio and were analyzed by the two-way ANOVA and a Bonferroni's multiple comparison test (**A-I**). **P<0.01 (by the Bonferroni's multiple comparison test). Representative blots of p-CREB (46 kDa), BDNF (14 kDa), p-TrkB (140 kDa) and β-actin (42 kDa) in the hippocampi of mice (**J**).

Statistical details:

(A) interaction [F(1,21)=13.97, p=0.0012], VPA 150 [F(1,21)=3.571, p= 0.0727], PTZ kindling [F(1,21)=0.3123, p=0.5822]; n=7 in each group, sample loss due to technical failure, thus the analysis based on n=7 VEH VEH, n=7 VPA 150 VEH, n=5 VEH PTZ, n=6 VPA 150 PTZ

(B) interaction [F(1,23)=0.0631, p=0.8039], VPA 150 [F(1,23)=0.06271, p=0.8045], PTZ kindling [F(1,23)=2.994, p=0.097]; n=7 in each group

(C) interaction [F(1,24)=6.205, p=0.02], VPA 150 [F(1,34)=1.873, p=0.1838], PTZ kindling [F(1,24)=2.282, p=0.144]; n=7 in each group

(D) interaction [F(1,22)=3.064, p=0.094], TC-G 1008 10 [F(1,22)=11.07, p=0.0031], PTZ kindling [F(1,22)=10.58, p=0.0037]; n=7 in each group, sample loss due to technical failure, thus the analysis based on n=7 VEH VEH, n=7 TC-G 1008 10 VEH, n=5 VEH PTZ, n=7 TC-G 1008 10 PTZ

(E) interaction [F(1,23)=0.1372, p=0.7145], TC-G 1008 10 [F(1,23)=0.3916, p=0.5376], PTZ kindling [F(1,23)=6.744, p=0.0161]; n=7 in each group

(F) interaction [F(1,24)=8.048, p=0.0091], TC-G 1008 10 [F(1,24)=0.2416, p=0.6275], PTZ kindling [F(1,24)=1.552, p=0.2249]; n=7 in each group

(G) interaction [F(1,22)=18.69, p=0.0003], Zn 8 [F(1,22)=2.542, p=0.1251], PTZ kindling [F(1,22)=0.4588, p=0.5053]; n=7 in each group, sample loss due to technical failure, thus the analysis based on n=7 VEH VEH, n=7 Zn 8 VEH, n=5 VEH PTZ, n=7 Zn 8 PTZ)

(H) interaction [F(1,22)= 1.934, p=0.1783], Zn 8 [F(1,22)=0.1052, p=0.7487], PTZ kindling [F(1,22)=13.36, p=0.0014]; n=7 in each group, sample loss due to technical failure, thus the analysis based on n=7 VEH VEH, n=7 Zn 8 VEH, n=7 VEH PTZ, n=6 Zn 8 PTZ

(I) interaction [F(1,24)=8.044, p=0.0091], Zn 8 [F(1,24)=0.07421, p=0.7876], PTZ kindling [F(1,24)=0.94, p=0.3419]; n=7 in each group

(**A-I** Two-way ANOVA)

PTZ kindling increased p-CREB (Fig 8A, D, G) and p-TrkB (Fig 8C, F, I) in the hippocampus of mice. Administration of TC-G 1008 (10 mg/kg) (Fig 8D), $ZnCl_2$ (8 mg Zn/kg) (Fig 8G) or VPA (150 mg/kg) (Fig 8A) decreased the level of p-CREB in the hippocampus of kindled mice. Administration of VPA (150 mg/kg) decreased the level of p-TrkB in the hippocampus of kindled mice (Fig 8C). Moreover, there was a tendency towards decreased p-TrkB level in the hippocampus of kindled mice after treatment with TC-G 1008 (10 mg/kg) (Fig 8F) or $ZnCl_2$ (8 mg Zn/kg) (Fig 8I).

The effects of GPR39 KO on the seizure threshold and development of PTZ kindling

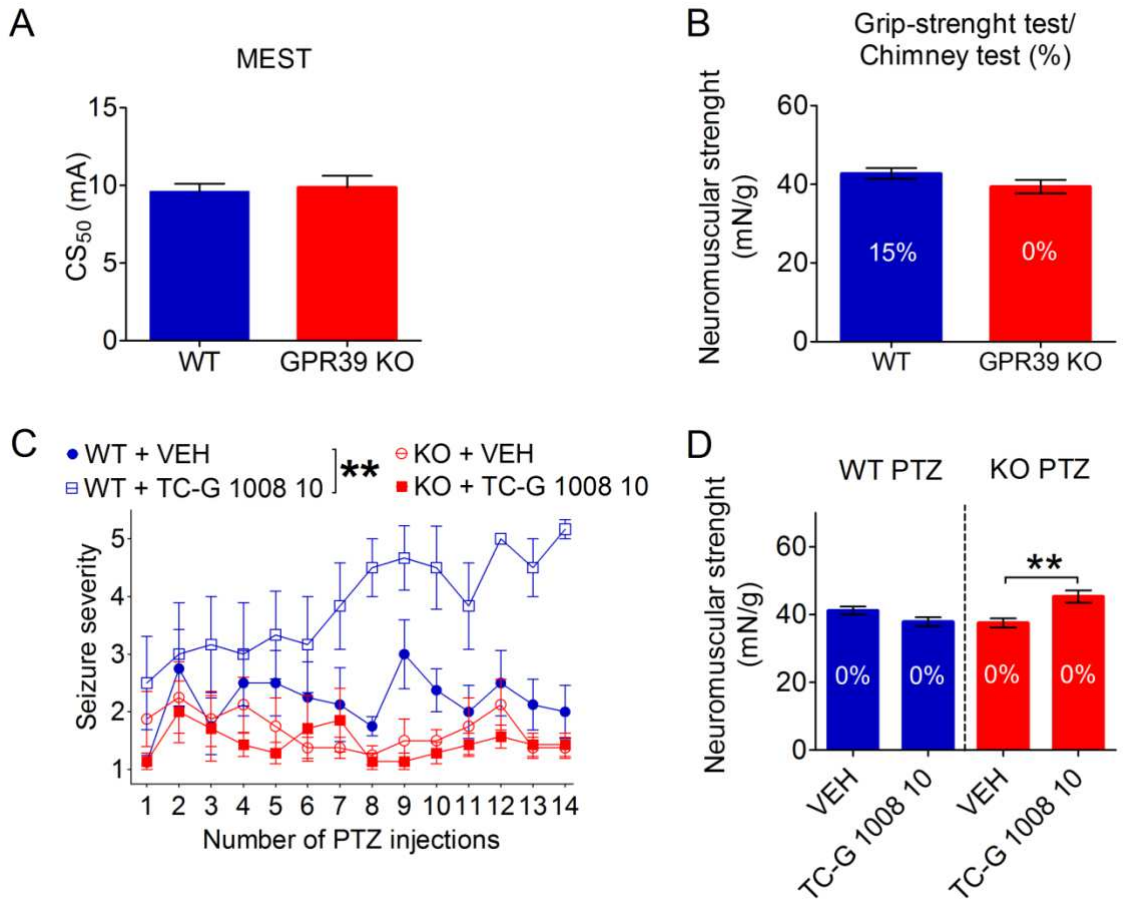

Fig 9. The effects of GPR39 KO in C57BL/6/Tar x CBA/Tar mice on the seizure threshold in the MEST test (**A**), on neuromuscular strength in the grip-strength test and on motor coordination in the chimney test (**B**). (**A**) Data are expressed as CS_{50} (in mA) with upper 95% confidence limits and were analyzed by the Student's t-test. (**B**) Neuromuscular strength (in the Grip-strength test) and motor coordination (in the chimney test) were assessed in experimentally naïve GPR39 KO and WT mice. Data from the grip-strength test (expressed as means ± SEM of the neuromuscular strength) and chimney test (expressed as % of animals which displayed impairment of motor coordination in this test) were analyzed by the Student's t-test or the Fisher's exact test, respectively. The effects of GPR39 KO and chronic treatment with TC-G 1008 on the development of PTZ kindling in C57BL/6/Tar x CBA/Tar mice (**C**). During PTZ kindling, WT and GPR39 KO mice were injected *i.p.* once daily with TC-G 1008 (10 mg/kg) or VEH (1% Tween 80 in 0.9 % NaCl) on every alternate day during weekdays. 30 min later, the mice were injected *i.p.* with PTZ (25 mg/kg). The total number of PTZ injections was 14. Data are expressed as means ± SEM of seizure severity and were analyzed by the three-way repeated measures ANOVA and the Bonferroni's multiple

comparison test. **P<0.01 (the Bonferroni's multiple comparison test). The effects of PTZ kindling in GPR39 KO or WT (C57BL/6/Tar x CBA/Tar) mice and chronic treatment with TC-G 1008 or VEH on neuromuscular strength in the grip-strength test and motor coordination in the chimney test (**D**). Neuromuscular strength and motor coordination were assessed on the last day of PTZ kindling in GPR39 KO or WT mice treated with TC-G 1008 (10 mg/kg) or VEH. Data from the grip-strength test (expressed as means ± SEM of the neuromuscular strength) were analyzed by the two-way ANOVA and the Bonferroni's multiple comparison test. Data from the chimney test are expressed as % of animals which displayed impairment of motor coordination in this test. **p<0.01 (the Bonferroni's multiple comparison test).

Statistical details:
(A) t(18)=1.19, p=0.2505, Student's t-test, n=20 in each group
(B) t(38)=1.521, p=0.1365, Student's t-test, n=20 in each group; p=0.2308 by the Fisher's exact test, n=20 in each group
(C) Genotype F(1, 25)=24.6011, p=0.000041; drug F(1, 25)=6.1898, p=0.019874; genotype x drug F(1, 25)=10.2347, p=0.003723; time F(13, 325)=1.7759, p=0.045707, time x genotype F(13, 325)=2.6197, p=0.001746; Three-way repeated measures ANOVA, n=8 WT VEH, n=7 WT TC-G 1008, n=8 KO VEH, n=7 KO TC-G 1008, 1 mouse was identified as outlier in WT TC-G 1008 group, thus excluded from the analysis
(**D**) genotype x treatment [F(1,26)=15.3, p=0.0006], genotype [F(1,24)=1.773, p=0.1946], treatment [F(1,24)=2.474, p=0.1278], Two-way AVOVA, n=8 WT VEH, n=7 WT TC-G 1008, n=8 KO VEH, n=7 KO TC-G 1008.

GPR39 KO mice do not differ from WT mice in terms of the seizure threshold in the MEST test

The seizure threshold did not differ between the GPR39 KO and WT mice in the MEST test (Fig 9A). Neuromuscular strength or motor coordination did not differ significantly between these groups of mice (Fig 9B).

TC-G 1008 facilitates the development of PTZ kindling in WT but not in GPR39 KO mice

The maximal seizure severity did not differ between the GPR39 KO and WT mice in the PTZ-kindling model. Chronic administration of TC-G 1008 increased the maximal seizure score in WT mice. Such effect was not observed in GPR39 KO mice (Fig 9C). After 14

injections of PTZ, the % of fully kindled mice was 25% in case of WT VEH group, 83.3% in case of WT TC-G 1008 10 group, 0% in case of KO VEH and 0% in case of KO TC-G 1008 group (Fisher's exact test p=0.0210 regarding WT TC-G 1008 group). To reduce possible mortality in WT mice treated with TC-G 1008 (10 mg/kg), exhibiting consecutive stage 5 seizures, kindling was terminated after 14 injections.

Furthermore, TC-G 1008 increased the neuromuscular strength in GPR39 KO mice subjected to PTZ kindling, but not in WT mice subjected to this procedure (Fig 9D).

The effects of chronic treatment with TC-G 1008 and PTZ-kindling in GPR39 KO or WT mice on $[Zn^{2+}]_I$, p-CREB, BDNF and p-TrkB in the hippocampus and on total serum zinc

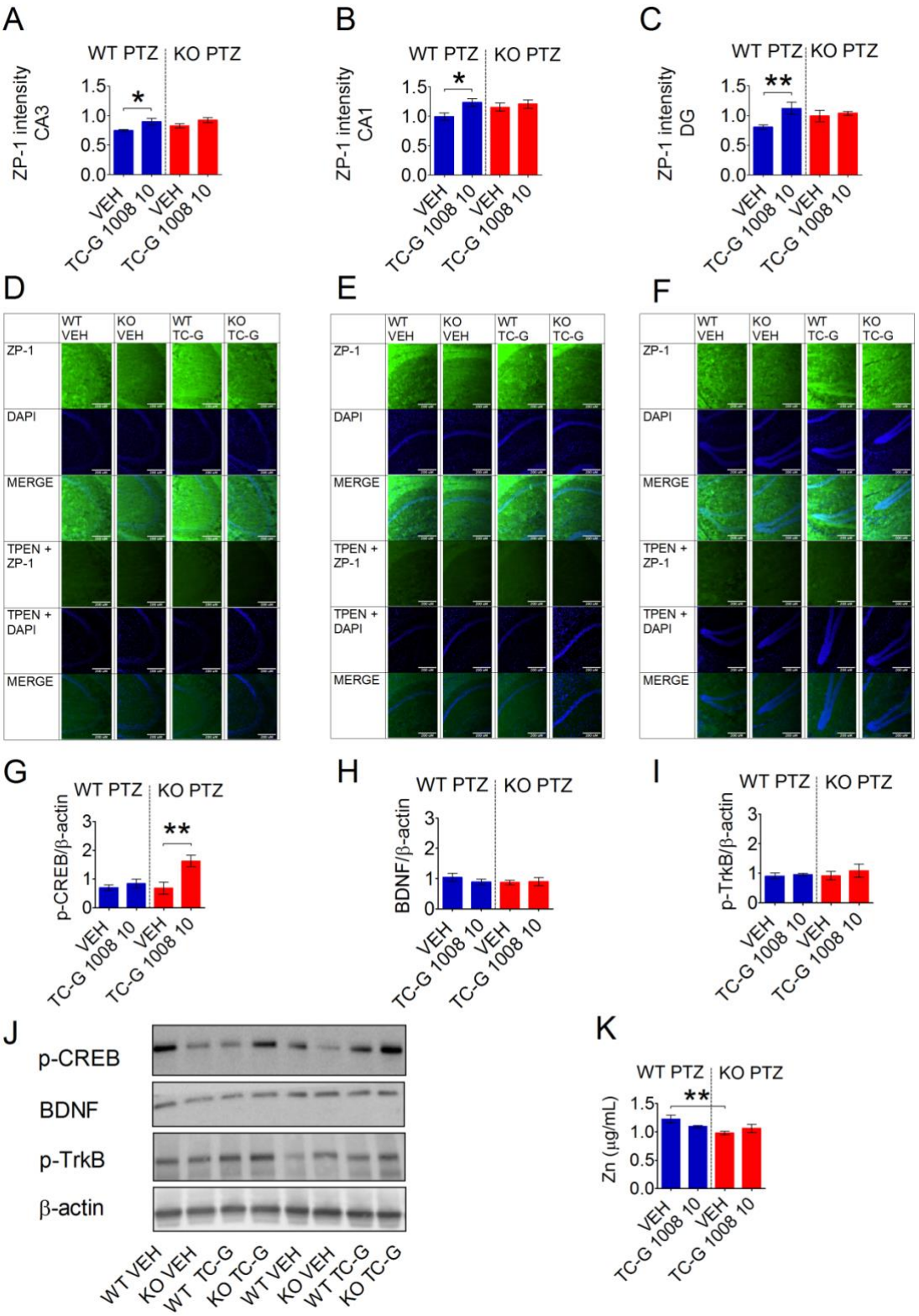

Fig 10. The effects of PTZ kindling in GPR39 KO or WT (C57BL/6/Tar x CBA/Tar) mice and chronic treatment with TC-G 1008 or VEH on $[Zn^{2+}]_I$ in the hippocampus (**A-F**), on the relative expression of proteins: p-CREB, BDNF or p-TrkB in the hippocampus (**G-I**) and on total serum zinc concentration (**K**). The PTZ kindling in GPR39 KO or WT (C57BL/6/Tar x CBA/Tar) mice consisted of 14 injections of PTZ (25 mg/kg). The biochemical analyses were performed at 24 h after the last PTZ injection. The ratio of mean ZP-1 grey values between mouse sections from WT or GPR39 KO mice that received either TC-G 1008 or VEH and underwent PTZ kindling, was analyzed in the CA3 (**A**), CA1 (**B**) or DG (**C**) regions of the hippocampus. Data were analyzed by the two-way ANOVA and the Bonferroni's multiple comparison test. *P<0.05, **p<0.01 (by the Bonferroni's multiple comparison test). Magnification of ZP-1 (green), DAPI (blue) and TPEN / ZP-1 in the CA3 (**D**), CA1 (**E**) and DG (**F**) is shown. Merged images include ZP-1 (green) or TPEN / ZP-1 and DAPI (blue). ZP-1 fluorescence is mostly absent in TPEN-treated section, thus revealing the high specificity of the Zn^{2+}-staining in brain sections. Scale bar=200 μM. The relative expression of proteins: p-CREB (**G**), BDNF (**H**) or p-TrkB (**I**) in the hippocampi. The results (mean ± SEM) are presented as the p-CREB or BDNF or p-TrkB/β-actin ratio and were analyzed by the two-way ANOVA and a Bonferroni's multiple comparison test. **P<0.01 (by the Bonferroni's multiple comparison test). Representative blots of p-CREB (46 kDa), BDNF (14 kDa), p-TrkB (140 kDa) and β-actin (42 kDa) in the hippocampi of mice (**J**). Total serum zinc concentration was measured by ICP-OES (**K**). Data are expressed as means ± SEM and were analyzed by the two-way ANOVA and a Bonferroni's multiple comparison test. **P<0.01 (by the Bonferroni's multiple comparison test).

Statistical details:

(A) genotype x treatment [F(1,19)=0.47, p=0.501], treatment [F(1,19)=8.88, p=0.0077], genotype [F(1,19)=1.66, p=0.2134]; n=6 WT VEH, n=6 WT TC-G 1008, n=5 KO VEH, n=6 KO TC-G 1008

(B) genotype x treatment [F(1,19)=1.97, p=0.1764], treatment [F(1,19)=4.91, p=0.0392], genotype [F(1,19)=1.04, p=0.3197]; n=6 WT VEH, n=6 WT TC-G 1008, n=5 KO VEH, n=6 KO TC-G 1008

(C) genotype x treatment [F(1,19)=3.59, p=0.0736], treatment [F(1,19)=6.41, p=0.0203], genotype [F(1,19)=0.54, p=0.4729]; n=6 WT VEH, n=6 WT TC-G 1008, n=5 KO VEH, n=6 KO TC-G 1008

(G) genotype x treatment [F(1,24=5.52, p=0.0224], treatment [F(1,24=10.07, p=0.0329], genotype [F(1,24=5.13, p=0.0329], n=7 in each group

(H) genotype x treatment [F(1,20=0.65, p=0.4288], treatment [F(1,20=0.26, p=0.6131]; genotype [F(1,20=0.44, p=0.5166], n=6 in each group

(**I**) genotype x treatment [F(1,24=0.18, p=0.6784], treatment [F(1,24=0.58, p=0.6131]; genotype [F(1,24=0.25, p=0.6250], n=7 in each group
(**K**) genotype x treatment [F(1,24)=3.56, p=0.0713], genotype [F(1,24)=6.00, p=0.0220], treatment [F(1,24)=0.17, p=0.6813], n=8 WT VEH, n=7 WT TC-G 1008, n=8 KO VEH, n=7 KO TC-G 1008, outliers excluded in KO VEH and WT TC-G 1008 groups, thus the analysis based on n=8 WT VEH, n=6 WT TC-G 1008, n=7 KO VEH, n=7 KO TC-G 1008
(A-C, G-I, K Two-way ANOVA)

Chronic treatment with TC-G 1008 increases $[Zn^{2+}]_I$ in the hippocampus of WT mice subjected to PTZ kindling

$[Zn^{2+}]_I$ intensity did not difer significanly between GPR39 KO and WT mice subjected to PTZ-kindling model (Fig 10 A-C), which consisted of 14 injections of PTZ (25 mg/kg). Chronic treatment with TC-G 1008 increased $[Zn^{2+}]_I$ in the CA3 (Fig 10A), CA1 (Fig 10B) and DG (Fig 10C) regions of the hippocampus of WT mice, but not of GPR39 KO mice subjected to this model.

Chronic treatment with TC-G 1008 increases p-CREB in the hippocampus of GPR39 KO mice subjected to PTZ kindling

The expression levels of p-CREB, BDNF or p-TrkB did not differ significantly between GPR39 KO and WT mice that were subjected to PTZ-kindling (Fig 10G-I). Chronic administration of TC-G 1008 markedly increased the expression of p-CREB protein in the hippocampus (by 137%) of GPR39 KO mice but not in WT mice (Fig 10G).

The effects of chronic treatment with TC-G 1008 on serum zinc concentration in GPR39 KO or WT mice subjected to PTZ kindling are not parallel to its effects on hippocampal $[Zn^{2+}]_I$

Serum zinc concentration was lower in VEH-treated GPR39 KO mice subjected to the PTZ kindling, compared with VEH-treated WT mice subjected to the PTZ kindling. Chronic

administration of TC-G 1008 did not affect serum zinc concentration in either GPR39 KO or WT mice subjected to this procedure (Fig 10H).

Discussion and Conclusions:

To examine *in vivo* signaling at GPR39, we used a specific agonist of this receptor, compound TC-G 1008. First, we showed that the concentrations of TC-G 1008 attained in the brain following *i.p.* administration in mice are sufficient to occupy GPR39. Previously there was no proof that TC-G 1008 is brain-penetrant. The compound aggravated acute PTZ-induced seizures in zebrafish, as shown with EEG assay and facilitated the development of PTZ-kindling in mice. The effects of TC-G 1008 in the chronic PTZ-induced model of epilepsy in WT C57BL/6/Tar x CBA/Tar mice were similar to those observed in Swiss Albino mice, while TC-G 1008 had no effect in GPR39 KO mice. Thus, by combining the observation on behavioral effects of TC-G 1008 in non-genetically modified mice and GPR39 KO mice we found that TC-G 1008 facilitates PTZ-induced epileptogenesis *via* GPR39 receptor. Noteworthy is the fact that we verified using GPR39 KO mice that GPR39 is a target for TC-G 1008 in this model. As one of the first pharmacological tool compounds for GPR39, TC-G 1008 has been used extensively to characterize the function of the receptor [13] but no study up to date has demonstrated *in vivo* that the effects of TC-G 1008 are mediated by GPR39. The compound was initially described as selective for GPR39 [21], but a further study suggested that it is a specific one as it may also bind to the serotonin 5HT1A receptor [22]. It is therefore crucial to evince that the effects obtained with TC-G 1008 are GPR39-dependent.

The GPR39 KO mice did not differ from WT mice in terms of the seizure threshold in the MEST test or the maximal seizure severity in the PTZ model. Thus, the genotype had no impact on either acute electrical seizures or epileptogenesis. However, TC-G 1008 facilitated the PTZ-epileptogenesis by acting at GPR39, thereby showing for the first time that activation of GPR39 aggravates epileptogenesis. This finding might have important therapeutic implications. Drug discovery efforts have focused on GPR39 [37-40] and GPR39 agonism

was suggested as a novel pharmacological strategy [22, 41]. GPR39 agonism might be beneficial in certain diseases, *e.g.*, depression [15, 42, 43] but it might also increase the risk of seizures.

In previous study GPR39 KO mice bred on C57BL/6 genetic background displayed higher maximal seizure severity score in response to an *i.p.* injection of a single dose of KA (10 mg/kg) [17, 18]. Our GPR39 KO model was established in mixed genetic background C57BL/6/Tar x CBA/Tar. The genetic background may account for seizure susceptibility [44]. The dose of KA used in the study of Gilad *et al.*, 2015 produced stage 5 seizures (loss of posture or status epilepticus) in 27% of the WT mice. Because we hypothesized that GPR39 agonist may protect from seizures induced by KA, we examined the effects of TC-G 1008 and $ZnCl_2$ on seizures induced by a single dose of KA of 40 mg/kg *i.p.* This dose of KA previously produced severe seizures in all examined mice [27]. $ZnCl_2$ increased the maximal seizure severity in response to KA (40 mg/kg) and both $ZnCl_2$ and TC-G 1008 decreased the latency to scratching. Thus, aggravation of acute KA-induced seizures was observed in both GPR39 KO mice and mice administered with TC-G 1008. However, in acute KA-seizure model we cannot exclude the involvement of other targets such as 5-HT1A in the activity of TC-G 1008 or $ZnCl_2$.

We examined both acute and chronic effects of the administered compounds and models of acute seizures or chronic PTZ-induced model of epilepsy on hippocampal $[Zn^{2+}]_I$ and expression of proteins of GPR39 signaling pathway. We chose the doses of compounds used in MES or 6-Hz seizure models based on the outcome of the respective seizure-threshold tests and we terminated PTZ kindling based on the seizure score for the group which displayed the highest seizure score, i.e., either TC-G 1008 or TC-G 1008 in WT mice group. As consequence, the doses of compounds used for biochemical analysis vary between MES and 6-Hz seizure model and the total number of PTZ injections (as well as the dose of PTZ)

differ between kindling in non-genetically modified and GPR39 KO mice, thus affecting the biochemical outcomes.

We performed the analysis of $[Zn^{2+}]_I$ in the DG, CA1 and CA3 regions of the hippocampus because they display high level of GPR39 mRNA expression [45] and high levels of zinc [46]. We observed that administration of TC-G 1008 at a low dose, which was ineffective in the MEST test, in mice subjected to MES seizures, was accompanied by decreased $[Zn^{2+}]_I$ in the CA1 and CA3 regions of the hippocampus. Moreover, administration of TC-G 1008 or $ZnCl_2$ at doses which were effective in the 6-Hz-threshold test, in mice subjected to 6-Hz seizures, was accompanied by decreased $[Zn^{2+}]_I$ in the CA1 and DG regions. Thus, the distinct effects of TC-G 1008 in the MEST and 6-Hz seizure threshold tests, *i.e*, either seizure threshold decreasing or increasing effects, respectively, might be associated with hippocampal $[Zn^{2+}]_I$.

Undoubtedly, the relationship between zinc signaling and seizures/epilepsy is complex as both extracellular zinc and $[Zn^{2+}]_I$ may produce either protective or detrimental effects by interacting with a variety of targets, raising the question how changes in extracellular zinc/ $[Zn^{2+}]_I$ concentrations influence its molecular targets and which of the effects will be prevailing [8]. Possible mechanisms linking GPR39, $[Zn^{2+}]_I$ and seizures/epilepsy include potassium-chloride co-transporter 2 (KCC2) [8]. KCC2 maintains low intracellular chloride concentration and is indispensable for inhibitory function of $GABA_A$ receptor [47]. Activation of GPR39 by extracellular zinc induced up-regulation of KCC2 [17, 18] and inhibited the release of the main excitatory neurotransmitter glutamate [48]. Conversely, an increased $[Zn^{2+}]_I$ inhibited KCC2 activity [49]. Therefore, $[Zn^{2+}]_I$ may play a key role in mediating the balance between neuronal inhibition/ excitation.

Previous semi-quantitative studies using fluorescent, cell membrane permeable probes demonstrated the association between $[Zn^{2+}]_I$ and SE. Staining with TFL-Zn of hippocampal

slices from pilocarpine-treated rats for zinc showed increased staining in the CA1 region, which appeared 1 day after SE and declined 2–4 days after [7]. Moreover, staining of hippocampal sections with TFL-Zn revealed that zinc accumulated in CA1 and CA3 neurons after KA-induced seizures [27]. In addition, the transient receptor potential melastatin 7 (TRPM7) inhibitor, carvacrol reduced the number of TSQ-positive neurons in the lithium chloride-pilocarpine-induced SE model [50]. The increase in $[Zn^{2+}]_I$ in the hippocampus of WT mice that underwent PTZ kindling and treatment with TC-G 1008 might be indicative of the relationship between $[Zn^{2+}]_I$ and enhanced epileptogenesis. The lack of significant differences in $[Zn^{2+}]_I$ in PTZ-kindled Swiss Albino mice that received TC-G 1008 may be explained by the dose of PTZ and the number of injections compared to those used in C57BL/6/Tar x CBA/Tar mice.

Serum zinc level has been suggested as a biomarker in epilepsy [51]. Furthermore, VPA was reported to decrease serum zinc [8, 52]. Here, serum zinc increased either after acute or chronic administration of $ZnCl_2$ but not after treatment with TC-G 1008, which is consistent with the observation that plasma zinc responds to zinc supplementation [53] and with a previous study which did not show changes in serum zinc concentration after a 2-week administration of TC-G 1008 [42]. Serum $[Zn^{2+}]_I$ (measured with ZP-1) was proposed to better reflect body's zinc status than total serum zinc but it did not correlate with the total serum concentration of zinc measured by ICP-MS [54]. Here, the changes in total serum zinc levels, as measured by the ICP-OES, were not parallel to changes observed in hippocampal $[Zn^{2+}]_I$.

We analyzed proteins which were previously shown to be associated with TC-G 1008 and GPR39 KO [43, 55], and are of interest in terms of seizures/ epileptogenesis, *i.e.*, p-CREB [56, 57], BDNF [58] and p-TrkB [59]. p-CREB expression was increased 3 min after seizures induced by *i.p.* administration of a single dose of PTZ (55 mg/kg) in the

hippocampus and cortex [60]. BDNF and p-TrkB increased in animal models and humans with epilepsy in the temporal and hippocampal areas. The inhibition of BDNF signaling was suggested as a strategy for the treatment of epilepsy [58]. However, the changes in protein expression did not correspond to the behavioral outcomes. For example, regarding acute seizures: in the 6-Hz seizure threshold test all compounds (TC-G 1008, $ZnCl_2$ and VPA) increased the seizure threshold while only VPA increased p-CREB in the hippocampus of mice subjected to the 6-Hz seizures (Fig S2). In the PTZ model in Swiss Albino mice TC-G 1008, $ZnCl_2$ and VPA facilitated, had no effect or suppressed epileptogenesis, respectively, but all compounds decreased the level of p-CREB in the hippocampus of kindled mice.

The increase in p-CREB protein level in the hippocampus of kindled GPR39 KO mice may be induced by TC-G 1008 acting at the 5-HT1A receptor [22]. The PRESTO-Tango GPCR-ome assay [61], which is based on measurement of G-protein independent β-arrestin, showed that TC-G 1008 may bind to 5-HT1A [22]. Also, zinc is an allosteric modulator of 5HT1A receptor, inducing a biphasic, concentration-dependent effect, either its activation (in sub-μM concentrations) or inhibition (in sub-mM concentrations) [62]. As GPR39, 5HT1A receptor belongs to GPCRs. The postsynaptic 5HT1A heteroreceptor is highly expressed in the hippocampus. Depending on the engagement of G protein subunits, 5HT1A activation may either increase cAMP level and subsequently increase phosphorylation of CREB or it may produce the opposite effects, *i.e.*, decrease cAMP and decrease CREB phosphorylation. In addition to G-proteins, 5HT1A signals via β-arrestin pathway [63]. Furthermore, 5HT1A and GPR39 may oligomerize [64]. Thus, our data implies that TC-G 1008 may bind to 5HT1A and affect CREB phosphorylation via this receptor. This finding might be important for the understanding of the literature accumulating in recent years on TC-G 1008 as a ligand of GPR39 [13], as some of the effects may have been induced by off-target(s).

In summary, the effects of TC-G 1008 in acute seizure models in mice or zebrafish may be attributable to its action at GPR39 or, presumably, 5HT1A, but our data consistently support the hypothesis that activation of GPR39 may aggravate epileptogenesis in the PTZ model, thus raising the possibility that antagonists of GPR39 shall be tested as antiepileptogenic drugs. Furthermore, we suggest that hippocampal $[Zn^{2+}]_I$ may mediate the acute effects of TC-G 1008 on MES and 6-Hz seizures.

Statements & Declarations

Funding: The study was supported by a grant from the National Science Centre, Poland (2016/20/S/NZ7/00424).

Competing interests: The authors have no relevant financial or non-financial interests to disclose.

Author contributions: All authors contributed to the study conception and design. Material preparation, data collection and analysis were performed by Urszula Doboszewska, Katarzyna Socała, Mateusz Pieróg, Dorota Nieoczym, Jan Sawicki, Małgorzata Szafarz, Kinga Gawel, Anna Rafalo-Ulińska, Elżbieta Wyska, Camila V. Esguerra, Bernadeta Szewczyk, Ireneusz Sowa, Piotr Wlaź. The first draft of the manuscript was written by Urszula Doboszewska and all authors commented on previous versions of the manuscript. All authors read and approved the final manuscript.

Data availability: The data that support the findings of this study are available from the corresponding author upon reasonable request.

Ethics approval: Housing and experimental procedures were conducted in accordance with the European Union Directive of 22 September 2010 (2010/63/EU) and Polish and Norwegian legislation acts concerning animal experimentation. The experiments in mice were approved by the Local Ethical Committee in Lublin (experiments in non-genetically modified mice: approval numbers 38/2017, 48/2018, 110/2018, 36/2019; experiments in GPR39 KO mice: approval numbers 72/2019, 16/2020), and the I Local Ethical Committee in Warsaw (approval number 811/2019 regarding generation of the GPR39 KO mouse line). The experiments in zebrafish were approved by the Norwegian Food Safety Authority experimental animal administration's supervisory and application system (“Forsøksdyrforvatningen tilsyns- og søknadssystem”; FOTS ID 15469 and 23935).

References

1. Ngugi AK, Bottomley C, Kleinschmidt I, Sander JW, Newton CR (2010) Estimation of the burden of active and life-time epilepsy: a meta-analytic approach. Epilepsia 51:883-890.

2. Dalic L, Cook MJ (2016) Managing drug-resistant epilepsy: challenges and solutions. Neuropsychiatr Dis Treat 12:2605-2616.

3. Galanopoulou AS, Buckmaster PS, Staley KJ, Moshe SL, Perucca E, Engel J, Jr., Loscher W, Noebels JL, Pitkanen A, Stables J, White HS, O'Brien TJ, Simonato M (2012) Identification of new epilepsy treatments: issues in preclinical methodology. Epilepsia 53:571-582.

4. Loscher W (2020) The holy grail of epilepsy prevention: preclinical approaches to antiepileptogenic treatments. Neuropharmacology 167:107605.

5. Maret W (2017) Zinc in cellular regulation: the nature and significance of "zinc signals". Int J Mol Sci 18:2285.

6. Fountain NB (2000) Status epilepticus: risk factors and complications. Epilepsia 41 Suppl 2:S23-S30.

7. van Loo KM, Schaub C, Pitsch J, Kulbida R, Opitz T, Ekstein D, Dalal A, Urbach H, Beck H, Yaari Y, Schoch S, Becker AJ (2015) Zinc regulates a key transcriptional pathway for epileptogenesis via metal-regulatory transcription factor 1. Nat Commun 6:8688.

8. Doboszewska U, Mlyniec K, Wlaz A, Poleszak E, Nowak G, Wlaz P (2019) Zinc signaling and epilepsy. Pharmacol Ther 193:156-177.

9. Yasuda S, Miyazaki T, Munechika K, Yamashita M, Ikeda Y, Kamizono A (2007) Isolation of Zn^{2+} as an endogenous agonist of GPR39 from fetal bovine serum. J Recept Signal Transduct Res 27:235-246.

10. Holst B, Egerod KL, Schild E, Vickers SP, Cheetham S, Gerlach LO, Storjohann L, Stidsen CE, Jones R, Beck-Sickinger AG, Schwartz TW (2007) GPR39 signaling is stimulated by zinc ions but not by obestatin. Endocrinology 148:13-20.

11. Hershfinkel M, Moran A, Grossman N, Sekler I (2001) A zinc-sensing receptor triggers the release of intracellular Ca2+ and regulates ion transport. Proc Natl Acad Sci U S A 98:11749-11754.

12. Maret W (2001) Crosstalk of the group IIa and IIb metals calcium and zinc in cellular signaling. Proc Natl Acad Sci U S A 98:12325-12327.

13. Laitakari A, Liu L, Frimurer TM, Holst B (2021) The zinc-sensing receptor GPR39 in physiology and as a pharmacological target. Int J Mol Sci 22:3872.

14. Davis CM, Bah TM, Zhang WH, Nelson JW, Golgotiu K, Nie X, Alkayed FN, Young JM, Woltjer RL, Silbert LC, Grafe MR, Alkayed NJ (2021) GPR39 localization in the aging human brain and correlation of expression and polymorphism with vascular cognitive impairment. Alzheimers Dement (N Y) 7:e12214.

15. Sah A, Kharitonova M, Mlyniec K (2021) Neuronal correlates underlying the role of the zinc sensing receptor (GPR39) in passive-coping behaviour. Neuropharmacology 198:108752.

16. Xie S, Jiang X, Doycheva DM, Shi H, Jin P, Gao L, Liu R, Xiao J, Hu X, Tang J, Zhang L, Zhang JH (2021) Activation of GPR39 with TC-G 1008 attenuates neuroinflammation via SIRT1/PGC-1alpha/Nrf2 pathway post-neonatal hypoxic-ischemic injury in rats. J Neuroinflammation 18:226-02289.

17. Gilad D, Shorer S, Ketzef M, Friedman A, Sekler I, Aizenman E, Hershfinkel M (2015) Homeostatic regulation of KCC2 activity by the zinc receptor mZnR/GPR39 during seizures. Neurobiol Dis 81:4-13.

18. Khan MZ (2016) A possible significant role of zinc and GPR39 zinc sensing receptor in Alzheimer disease and epilepsy. Biomed Pharmacother 79:263-272.

19. Chen NN, Zhao DJ, Sun YX, Wang DD, Ni H (2019) Long-term effects of zinc deficiency and zinc supplementation on developmental seizure-induced brain damage and the underlying GPR39/ZnT-3 and MBP expression in the hippocampus. Front Neurosci 13:920.

20. Wasilewska I, Gupta RK, Wojtas B, Palchevska O, Kuznicki J (2020) stim2b knockout induces hyperactivity and susceptibility to seizures in zebrafish larvae. Cells 9:1285.

21. Peukert S, Hughes R, Nunez J, He G, Yan Z, Jain R, Llamas L, Luchansky S, Carlson A, Liang G, Kunjathoor V, Pietropaolo M, Shapiro J, Castellana A, Wu X, Bose A (2014) Discovery of 2-pyridylpyrimidines as the first orally bioavailable GPR39 agonists. ACS Med Chem Lett 5:1114-1118.

22. Sato S, Huang XP, Kroeze WK, Roth BL (2016) Discovery and characterization of novel GPR39 agonists allosterically modulated by zinc. Mol Pharmacol 90:726-737.

23. Socala K, Wlaz P (2021) Acute seizure tests used in epilepsy research: step-by-step protocol of the maximal electroshock seizure (MES) test, the maximal electroshock seizure threshold (MEST) test, and the pentylenetetrazole (PTZ)-induced seizure test in rodents. In: Vohora D (ed) Experimental and translational methods to screen drugs effective against seizures and epilepsy, Springer, New York, NY, USA, pp 79-102.

24. Kimball AW, Burnett WT, Jr., Doherty DG (1957) Chemical protection against ionizing radiation. I. Sampling methods for screening compounds in radiation protection studies with mice. Radiat Res 7:1-12.

25. Socala K, Nieoczym D, Pierog M, Wyska E, Szafarz M, Doboszewska U, Wlaz P (2018) Effect of tadalafil on seizure threshold and activity of antiepileptic drugs in three acute seizure tests in mice. Neurotox Res 34:333-346.

26. Khanam R, Vohora D (2021) Protocol for 6 Hz corneal stimulation in rodents for refractory seizures. In: Vohora D (ed) Experimental and translational methods to screen drugs effective against seizures and epilepsy, Springer, New York, NY, USA, pp 167-179.

27. Lee JY, Cole TB, Palmiter RD, Koh JY (2000) Accumulation of zinc in degenerating hippocampal neurons of ZnT3-null mice after seizures: evidence against synaptic vesicle origin. J Neurosci 20:RC79.

28. Iqbal R, Jain GK, Siraj F, Vohora D (2018) Aromatase inhibition by letrozole attenuates kainic acid-induced seizures but not neurotoxicity in mice. Epilepsy Res 143:60-69.

29. Cole TB, Robbins CA, Wenzel HJ, Schwartzkroin PA, Palmiter RD (2000) Seizures and neuronal damage in mice lacking vesicular zinc. Epilepsy Res 39:153-169.

30. Potschka H (2021) Procedures for electrical and chemical kindling models in rats and mice. In: Vohora D (ed) Experimental and translational methods to screen drugs effective against seizures and epilepsy, Springer, New York, NY, USA, pp 103-119.

31. Socala K, Mogilski S, Pierog M, Nieoczym D, Abram M, Szulczyk B, Lubelska A, Latacz G, Doboszewska U, Wlaz P, Kaminski K (2019) KA-11, a novel pyrrolidine-2,5-dione derived broad-spectrum anticonvulsant: its antiepileptogenic, antinociceptive properties and in vitro characterization. ACS Chem Neurosci 10:636-648.

32. Socala K, Doboszewska U, Wlaz P (2020) Salvinorin A does not affect seizure threshold in mice. Molecules 25:1204.

33. Afrikanova T, Serruys AS, Buenafe OE, Clinckers R, Smolders I, de Witte PA, Crawford AD, Esguerra CV (2013) Validation of the zebrafish pentylenetetrazol seizure model: locomotor versus electrographic responses to antiepileptic drugs. PLoS One 8:e54166.

34. Gawel K, Langlois M, Martins T, van der Ent W, Tiraboschi E, Jacmin M, Crawford AD, Esguerra CV (2020) Seizing the moment: zebrafish epilepsy models. Neurosci Biobehav Rev 116:1-20.

35. Nieoczym D, Socala K, Gawel K, Esguerra CV, Wyska E, Wlaz P (2019) Anticonvulsant activity of pterostilbene in zebrafish and mouse acute seizure tests. Neurochem Res 44:1043-1055.

36. Grabrucker AM, Schmeisser MJ, Udvardi PT, Arons M, Schoen M, Woodling NS, Andreasson KI, Hof PR, Buxbaum JD, Garner CC, Boeckers TM (2011) Amyloid beta protein-induced zinc sequestration leads to synaptic loss via dysregulation of the ProSAP2/Shank3 scaffold. Mol Neurodegener 6:65.

37. Grunddal KV, Diep TA, Petersen N, Tough IR, Skov LJ, Liu L, Buijink JA, Mende F, Jin C, Jepsen SL, Sorensen LME, Achiam MP, Strandby RB, Bach A, Hartmann B, Frimurer TM, Hjorth SA, Bouvier M, Cox H, Holst B (2021) Selective release of gastrointestinal hormones induced by an orally active GPR39 agonist. Mol Metab 49:101207.

38. Frimurer TM, Mende F, Graae AS, Engelstoft MS, Egerod KL, Nygaard R, Gerlach LO, Hansen JB, Schwartz TW, Holst B (2017) Model-based discovery of synthetic agonists for the Zn(2+)-sensing G-protein-coupled receptor 39 (GPR39) reveals novel biological functions. J Med Chem 60:886-898.

39. Fjellstrom O, Larsson N, Yasuda S, Tsuchida T, Oguma T, Marley A, Wennberg-Huldt C, Hovdal D, Fukuda H, Yoneyama Y, Sasaki K, Johansson A, Lundqvist S, Brengdahl J, Isaacs RJ, Brown D, Geschwindner S, Benthem L, Priest C, Turnbull A (2015) Novel Zn2+ modulated GPR39 receptor agonists do not drive acute insulin secretion in rodents. PLoS One 10:e0145849.

40. Bassilana F, Carlson A, DaSilva JA, Grosshans B, Vidal S, Beck V, Wilmeringwetter B, Llamas LA, Showalter TB, Rigollier P, Bourret A, Ramamurthy A, Wu X, Harbinski F, Plonsky S, Lee L, Ruffner H, Grandi P, Schirle M, Jenkins J, Sailer AW, Bouwmeester T, Porter JA, Myer V, Finan PM, Tallarico JA, Kelleher JF, III, Seuwen K, Jain RK, Luchansky SJ (2014) Target identification for a Hedgehog pathway inhibitor reveals the receptor GPR39. Nat Chem Biol 10:343-349.

41. Mlyniec K, Singewald N, Holst B, Nowak G (2015) GPR39 Zn^{2+}-sensing receptor: a new target in antidepressant development? J Affect Disord 174:89-100.

42. Starowicz G, Jarosz M, Frackiewicz E, Grzechnik N, Ostachowicz B, Nowak G, Mlyniec K (2019) Long-lasting antidepressant-like activity of the GPR39 zinc receptor agonist TC-G 1008. J Affect Disord 245:325-334.

43. Mlyniec K, Starowicz G, Gawel M, Frackiewicz E, Nowak G (2016) Potential antidepressant-like properties of the TC G-1008, a GPR39 (zinc receptor) agonist. J Affect Disord 201:179-184.

44. Schauwecker PE (2011) The relevance of individual genetic background and its role in animal models of epilepsy. Epilepsy Res 97:1-11.

45. Jackson VR, Nothacker HP, Civelli O (2006) GPR39 receptor expression in the mouse brain. Neuroreport 17:813-816.

46. Perez-Clausell J, Danscher G (1985) Intravesicular localization of zinc in rat telencephalic boutons. A histochemical study. Brain Res 337:91-98.

47. Moore YE, Kelley MR, Brandon NJ, Deeb TZ, Moss SJ (2017) Seizing control of KCC2: a new therapeutic target for epilepsy. Trends Neurosci 40:555-571.

48. Lu HC, Mackie K (2016) An introduction to the endogenous cannabinoid system. Biol Psychiatry 79:516-525.

49. Hershfinkel M, Kandler K, Knoch ME, Dagan-Rabin M, Aras MA, Abramovitch-Dahan C, Sekler I, Aizenman E (2009) Intracellular zinc inhibits KCC2 transporter activity. Nat Neurosci 12:725-727.

50. Jeong JH, Lee SH, Kho AR, Hong DK, Kang DH, Kang BS, Park MK, Choi BY, Choi HC, Lim MS, Suh SW (2020) The transient receptor potential melastatin 7 (TRPM7) inhibitors suppress seizure-induced neuron death by inhibiting zinc neurotoxicity. Int J Mol Sci 21:7897.

51. Scassellati C, Bonvicini C, Benussi L, Ghidoni R, Squitti R (2020) Neurodevelopmental disorders: metallomics studies for the identification of potential biomarkers associated to diagnosis and treatment. J Trace Elem Med Biol 60:126499.

52. Jia W, Song Y, Yang L, Kong J, Boczek T, He Z, Wang Y, Zhang X, Hu H, Shao D, Tang H, Xia L, Xu X, Guo F (2020) The changes of serum zinc, copper, and selenium levels in epileptic patients: a systematic review and meta-analysis. Expert Rev Clin Pharmacol 13:1047-1058.

53. King JC, Brown KH, Gibson RS, Krebs NF, Lowe NM, Siekmann JH, Raiten DJ (2015) Biomarkers of nutrition for development (BOND)-zinc review. J Nutr 146:858S-885S.

54. Alker W, Schwerdtle T, Schomburg L, Haase H (2019) A zinpyr-1-based fluorimetric microassay for free zinc in human serum. Int J Mol Sci 20:4006.

55. Mlyniec K, Budziszewska B, Holst B, Ostachowicz B, Nowak G (2014) GPR39 (zinc receptor) knockout mice exhibit depression-like behavior and CREB/BDNF down-regulation in the hippocampus. Int J Neuropsychopharmacol 18:1-8.

56. Mertz C, Krarup S, Jensen CD, Lindholm SEH, Kjaer C, Pinborg LH, Bak LK (2020) Aspects of cAMP signaling in epileptogenesis and seizures and its potential as drug target. Neurochem Res 45:1247-1255.

57. Wang G, Zhu Z, Xu D, Sun L (2020) Advances in understanding CREB signaling-mediated regulation of the pathogenesis and progression of epilepsy. Clin Neurol Neurosurg 196:106018.

58. Iughetti L, Lucaccioni L, Fugetto F, Predieri B, Berardi A, Ferrari F (2018) Brain-derived neurotrophic factor and epilepsy: a systematic review. Neuropeptides 72:23-29.

59. Lin TW, Harward SC, Huang YZ, McNamara JO (2020) Targeting BDNF/TrkB pathways for preventing or suppressing epilepsy. Neuropharmacology 167:107734.

60. Moore AN, Waxham MN, Dash PK (1996) Neuronal activity increases the phosphorylation of the transcription factor cAMP response element-binding protein (CREB) in rat hippocampus and cortex. J Biol Chem 271:14214-14220.

61. Kroeze WK, Sassano MF, Huang XP, Lansu K, McCorvy JD, Giguere PM, Sciaky N, Roth BL (2015) PRESTO-Tango as an open-source resource for interrogation of the druggable human GPCRome. Nat Struct Mol Biol 22:362-369.

62. Satala G, Duszynska B, Stachowicz K, Rafalo A, Pochwat B, Luckhart C, Albert PR, Daigle M, Tanaka KF, Hen R, Lenda T, Nowak G, Bojarski AJ, Szewczyk B (2016) Concentration-dependent dual mode of Zn action at serotonin 5-HT_{1A} receptors: in vitro and in vivo studies. Mol Neurobiol 53:6869-6881.

63. Salaciak K, Pytka K (2021) Biased agonism in drug discovery: is there a future for biased 5-HT(1A) receptor agonists in the treatment of neuropsychiatric diseases? Pharmacol Ther 227:107872.

64. Mlyniec K, Siodlak D, Doboszewska U, Nowak G (2021) GPCR oligomerization as a target for antidepressants: focus on GPR39. Pharmacol Ther 225:107842.

Supplemental data

Table S1. Pharmacokinetic parameters of TC-G 1008 in mice estimated using the non-compartmental analysis following administration of this compound at a single dose of 20 mg/kg, *i.p.*

Parameter	Serum	Brain
t_{max} (min)	15	15
C_{max} (ng/mL)	2930	36.32
λ_z (min^{-1})	0.015	0.014
$t_{0.5\,\lambda z}$ (min)	47.77	50.18
V_z/F (L/kg)	6.47	-
CL/F (L/min/kg)	0.97	-
AUC_{0-t} (ng·min/mL)	172860	2309
$AUC_{0-\infty}$ (ng·min/mL)	213045.4	2911.6
MRT (min)	73.18	77.50

C_{max} – maximum serum concentration, t_{max} – time to reach maximum concentration, λ_z – terminal slope, $t_{0.5\lambda z}$ – terminal half-life, AUC_{0-t} – area under the concentration-time curve from the time of dosing to the last measured point, $AUC_{0-\infty}$ – area under the concentration-time curve from the time of dosing to infinity, V_z – volume of distribution based on the terminal phase, CL – clearance, F – fraction absorbed, MRT – mean residence time.

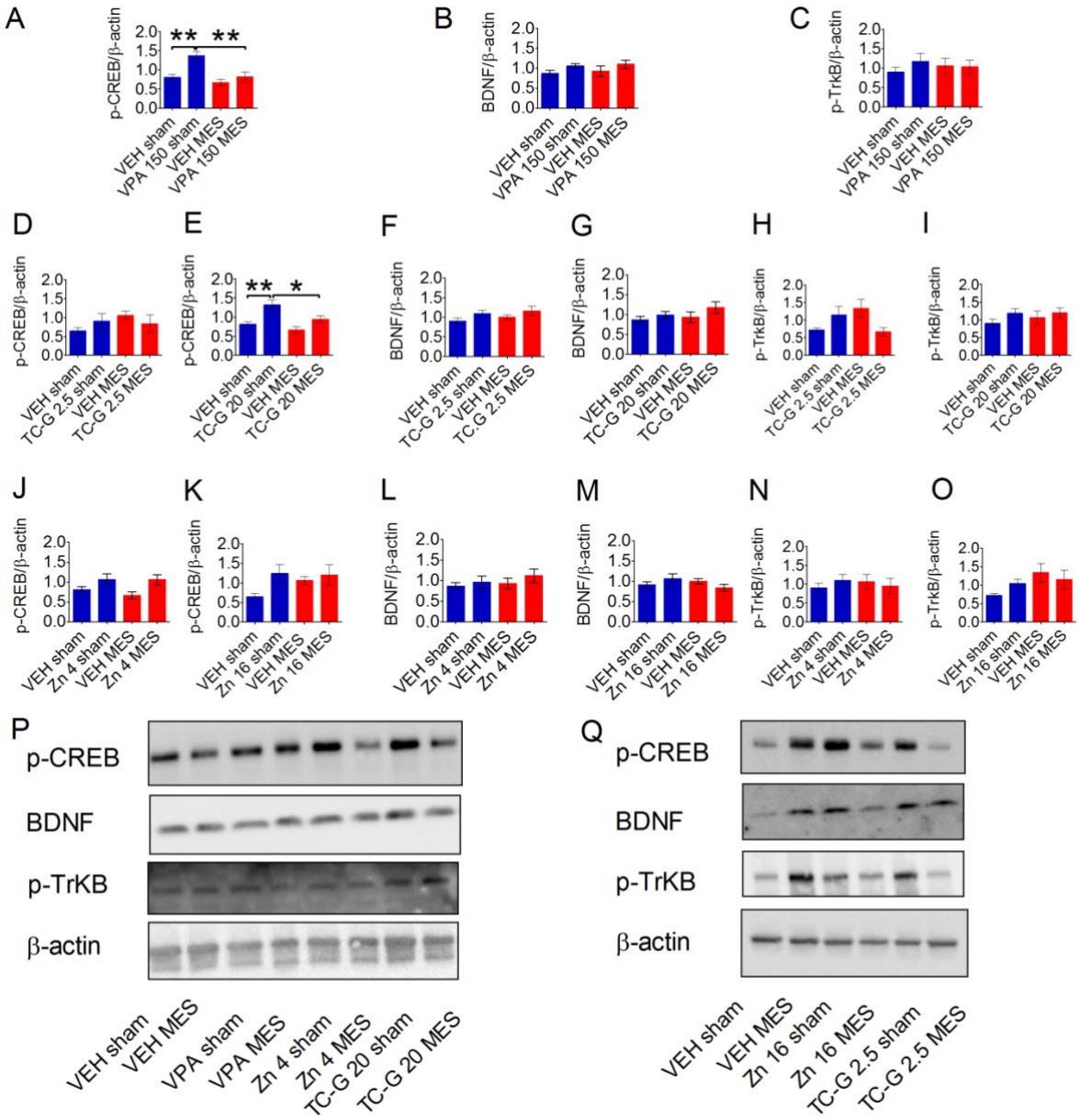

Fig S1. The effects of single doses of VPA, TC-G 1008 or $ZnCl_2$ and maximal electroshock seizure (MES) generated by supramaximal current intensity of 50 mA on the relative expression of proteins: phosphorylated CREB at Ser 133 (p-CREB), BDNF or phosphorylated TrkB at Tyr 816 (p-TrkB) in the hippocampi of Swiss Albino mice. Drugs or VEH (1% Tween 80 in 0.9% NaCl) were administered *i.p.* 30 min before MES. Non-stimulated (sham) animals received the respective doses of drugs or VEH but they did not receive an electrical stimulus. The results (mean ± SEM) are presented as the p-CREB or BDNF or p-TrkB/β-actin ratio and were analyzed by the two-way ANOVA and the Bonferroni's multiple comparison test (**A-O**). *P<0.05, **p<0.01 (the Bonferroni's multiple comparison test). Representative

blots of p-CREB (46 kDa), BDNF (14 kDa), p-TrkB (140 kDa) and β-actin (42 kDa) in the hippocampi of mice (**P, Q**).

Statistical details:

(A) interaction [F(1,22)=3.979, p=0.0586], VPA 150 [F(1,22)=12.35, p= 0.002], MES [F(1,22)=11.51, p=0.0026]; n=7 in each group, samples damaged due to technical failure or outlier excluded, thus the analysis based on n=6 VEH sham, n=7 VPA 150 sham, n=6 VEH MES, n=7 VPA 150 MES

(B) interaction [F(1,24)=0.007895, p=0.9299], VPA 150 [F(1,24)=3.365, p= 0.079], MES [F(1,24)=0.2656, p=0.611]; n=7 in each group

(C) interaction [F(1,22)=0.7707, p=0.3895], VPA 150 [F(1,22)=0.5319, p=0.4735], MES [F(1,22)=0.00304, p=0.9565]; n=7 in each group, samples damaged due to technical failure excluded, thus the analysis based on n=7 VEH sham, n=7 VPA 150 sham, n=6 VEH MES, n=6 VPA 150 MES

(D) interaction [F(1,28)=1.952, p=0.1733], TC-G 1008 2.5 [F(1,28)= 0.008663, p=0.9265], MES [F(1,28)=1.057, p=0.3128]; n=8 in each group

(E) interaction [F(1,21)=1.351, p=0.2582], TC-G 1008 20 [F(1,21)= 15.34, p=0.0008], MES [F(1,21)=6.668, p=0.0174]; n=7 in each group, samples damaged due to technical failure or outliers excluded, thus the analysis based on n=6 VEH sham, n=6 TC-G 1008 20 sham, n=6 VEH MES, n=7 TC-G 1008 20 MES

(F) interaction [F(1,28)=0.3767, p=0.5443], TC-G 1008 2.5 [F(1,28)=5.93, p=0.0215], MES [F(1,28)=2.102, p=0.1582]; n=8 in each group

(G) interaction [F(1,24)=0.3232, p=0.575], TC-G 1008 20 [F(1,24)=2.355, p=0.1379], MES [F(1,24)=1.165, p=0.2911]; n=7 in each group

(**H**) interaction [F(1,26)=8.503, p=0.0072], TC-G 1008 2.5 [F(1,26)=0.06207, p=0.8052], MES [F(1,26)= 0.1442, p= 0.7073]; n=8 in each group, samples damaged due to technical failure excluded, thus the analysis based on n=8 VEH sham, n=7 TC-G 1008 2.5 sham, n=8 VEH MES, n=7 TC-G 1008 2.5 MES

(I) interaction [F(1,22)=02262, p=0.639], VPA 150 [F(1,22)=1.883, p= 0.1839], MES [F(1,22)=0.361, p=0.5541]; n=7 in each group, samples damaged due to technical failure excluded, thus the analysis based on n=7 VEH sham, n=6 TC-G 1008 20 sham, n=6 VEH MES, n=7 TC-G 1008 20 MES

(J) interaction [F(1,22)=0.378, p=0.545], Zn 4 [F(1,22)=7.659, p=0.0112], MES [F(1,22)=0.3675, p=0.5506]; n=7 in each group, samples damaged due to technical failure during WB or outliers excluded, thus the analysis based on n=6 VEH sham, n=7 Zn 4 sham, n=6 VEH MES, n=7 Zn 4 MES

(K) interaction [F(1,28)=1.498, p=0.2311], Zn 16 [F(1,28)=4.021, p=0.0547], MES [F(1,28)=0.9988, p=0.3262]; n=8 in each group

(L) interaction [F(1,24)=0.2363, p=0.6313], Zn 4 [F(1,24)=0.8156, p=0.3754], MES [F(1,24)=0.4332, p=0.5167]; n=7 in each group

(M) interaction [F(1,28)=6.043, p=0.0204], Zn 16 [F(1,28)=0.2976, p=0.5897], MES [F(1,28)=0.06256, p=0.8043] n=8 in each group

(N) interaction [F(1,23)=0.8277, p=03724], Zn 4 [F(1,23)=0.06636, p=0.799], MES [F(1,23)=0.001761, p=0.9669]; n=7 in each group, samples damaged due to technical failure

excluded, thus the analysis based on n=7 VEH sham, n=7 Zn 4 sham, n=6 VEH MES, n=7 Zn 4 MES
(O) interaction [F(1,26)=0.8987, p=0.3519], Zn 16 [F(1,26)=0.9681, p=0.3342], MES [F(1,26)=2.525, p=0.1242]; n=8 in each group, samples damaged due to technical failure excluded, thus the analysis based on n=8 VEH sham, n=7 Zn 16 sham, n=8 VEH MES, n=7 Zn 16 MES
(A-O Two-way ANOVA)

The level of p-CREB was significantly increased (in the case of TC-G 1008 20 mg/kg (Fig S1 E) or VPA 150 mg/kg (Fig S1 A)) or there were tendencies towards increased p-CREB protein level (in the case of TC-G 1008 2.5 mg/kg (Fig S1 D), Zn 4 mg Zn/kg (Fig S1 J) or Zn 16 mg/kg (Fig S1 K)) in the hippocampus of sham mice after administration of single doses of these compounds. There were also tendencies towards increased p-TrkB protein level in the hippocampus of sham mice after administration of single doses of TC-G 1008 (2.5 mg/kg (Fig S1 H) or 20 mg/kg (Fig S1 I)), $ZnCl_2$ (4 mg Zn/kg (Fig S1 N) or 16 mg Zn/kg (Fig S1 O)) or VPA (150 mg/kg (Fig S1 C)).

There were tendencies towards increased p-CREB protein levels in the hippocampus of mice that received MES. Mice that received MES after administration of TC-G 1008 20 mg/kg (Fig S1 E) or VPA 150 mg/kg (Fig S1 A) had decreased p-CREB in the hippocampus compared to sham mice that received the respective compounds.

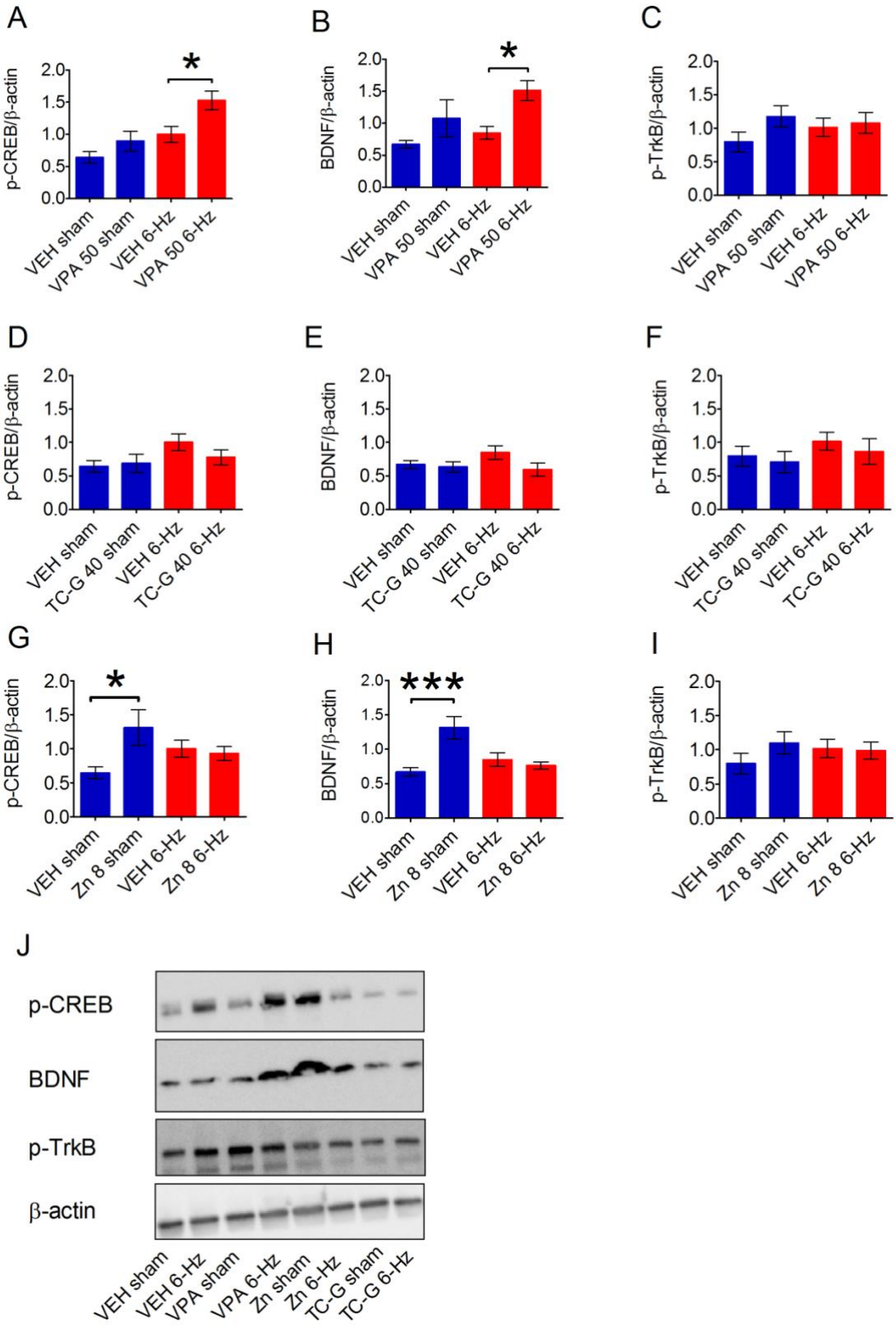

Fig S2. The effects of single doses of VPA, TC-G 1008 or $ZnCl_2$ and supramaximal current intensity of 32 mA (6-Hz seizure) on the relative expression of proteins: phosphorylated CREB at Ser 133 (p-CREB), BDNF or phosphorylated TrkB at Tyr 816 (p-TrkB) in the

hippocampi of Swiss Albino mice. Drugs or VEH (1% Tween 80 in 0.9 % NaCl) were administered *i.p.* 30 min before the 6-Hz seizure. Non-stimulated (sham) animals received the respective doses of drugs or VEH but they did not receive the electrical stimulus. The results (mean ± SEM) are presented as the p-CREB or BDNF or p-TrkB/β-actin ratio and were analyzed by the two-way ANOVA and a Bonferroni's multiple comparison test (**A-I**). *P<0.05, ***p<0.001 (the Bonferroni's multiple comparison test). Representative blots of p-CREB (46 kDa), BDNF (14 kDa), p-TrkB (140 kDa) and β-actin (42 kDa) in the hippocampi of Swiss Albino mice (**J**).

Statistical details:

(A) interaction [F(1,24)=1.125, p=0.2994], VPA 50 [F(1,24)=8.918, p=0.0064], 6-Hz [F(1,24)=14.36, p=0.0009]; n=7 in each group

(B) interaction [F(1,23)=0.5007, p=0.4863], VPA 50 [F(1,23)=8.737, p=0.0071], 6-Hz seizure [F(1,23)=2.859, p=0.1044]; n=7 in each group, outliers excluded, thus the analysis based on n=6 VEH sham, n=7 VPA 50 sham, n=7 VEH 6-Hz, n=7 VPA 50 6-Hz

(C) interaction [F(1,22)=1.078, p=0.3104], VPA 50 [F(1,22)=2.122, p=0.1593], 6-Hz seizure [F(1,22)=0.1582, p=0.6947]; n=7 in each group, samples damaged due to technical failure excluded, thus the analysis based on n=5 VEH sham, n=7 TC-G 1008 40 sham, n=7 VEH 6-Hz, n=7 TC-G 1008 40 6-Hz

(D) interaction [F(1,24)=1.309, p=0.2639], TC-G 1008 40 [F(1,24)= 0.576, p=0.4553], 6-Hz [F(1,24)=3.664, p=0.0676]; n=7 in each group

(E) interaction [F(1,23)=1.526, p=0.2292], TC-G 1008 40 [F(1,23)=2.708, p=0.1134], 6-Hz seizure [F(1,23)=0.5955, p=0.4482]; n=7 in each group, outliers excluded, thus the analysis based on n=6 VEH sham, n=7 TC-G 1008 40 sham, n=7 VEH 6-Hz, n=7 TC-G 1008 40 6-Hz

(F) interaction [F(1,22)=0.0349, p=0.8535], TC-G 1008 40 [F(1,22)=0.5357, p=0.8535], 6-Hz seizure [F(1,22)=1.322, p=0.2625]; n=7 in each group, samples damaged due to technical failure excluded, thus the analysis based on n=5 VEH sham, n=7 TC-G 1008 40 sham, n=7 VEH 6-Hz, n=7 TC-G 1008 40 6-Hz

(G) interaction [F(1,24)=5.388, p=0,0291], Zn 8 [F(1,24)=3.485, p=0,0742], 6-Hz [F(1,24)=0.0062, p=0.9381]; n=7 in each group

(**H**) interaction [F(1,23)=11,76, p=0.0023], Zn 8 [F(1,23)=6,87, p=0.0153], 6-Hz seizure [F(1,23)=3,113, p=0.0909]; n=7 in each group, outlier excluded, thus the analysis based on n=6 VEH sham, n=7 Zn 8 sham, n=7 VEH 6-Hz, n=7 Zn 8 6-Hz

(I) interaction [F(1,22)=1.286, p=0.2691], Zn 8 [F(1,22)=0.8649, p=0.3625], 6-Hz seizure [F(1,22)=0.1362, p=0.7156]; n=7 in each group, samples damaged due to technical failure excluded, thus the analysis based on n=5 VEH sham, n=7 TC-G 1008 40 sham, n=7 VEH 6-Hz, n=7 TC-G 1008 40 6-Hz

(A-I Two-way ANOVA)

Administration of $ZnCl_2$ (8 mg Zn/kg) increased p-CREB (Fig S2 G) and BDNF (Fig S2 G) protein levels in the hippocampus of sham mice. There were tendencies towards increased p-CREB protein levels in the hippocampus of mice that received VEH and 6-Hz

seizure, compared to VEH treated-sham mice. Administration of VPA (50 mg/kg) increased p-CREB (Fig S2 A) and BDNF (Fig S2 B) protein levels in the hippocampus of mice that received the 6-Hz seizure, compared to VEH.